




Article

Optimal Location and Sizing of Distributed Generators in Power System Network with Power Quality Enhancement Using Fuzzy Logic Controlled D-STATCOM

Prashant ¹, Anwar Shahzad Siddiqui ¹, Md Sarwar ^{1,*}, Ahmed Althobaiti ² and Sherif S. M. Ghoneim ^{2,*}

¹ Department of Electrical Engineering, Faculty of Engineering & Technology, Jamia Millia Islamia, New Delhi 110025, India; prashant.pacificcold@gmail.com (P.); assiddiqui@jmi.ac.in (A.S.S.)

² Electrical Engineering Department, College of Engineering, Taif University, P.O. Box 11099, Taif 21944, Saudi Arabia; ahmed.althobaiti@tu.edu.sa

* Correspondence: msarwar@jmi.ac.in (M.S.); s.ghoneim@tu.edu.sa (S.S.M.G.)

Abstract: This article presents the selection of location and sizing of multiple distributed generators (DGs) for boosting performance of the radial distribution system in the case of constant power load flow and constant impedance load flow. The consideration of placing and sizing of DGs is to meet the load demand. This article tries to overcome the limitations of existing techniques for determining the appropriate location and size of DGs. The selection of DG location is decided in terms of real power losses, accuracy, and sensitivity. The size of DG is measured in terms of real and reactive power. Both positioning and sizing of DG are analyzed with the genetic algorithm and the heuristic probability distribution method. The results are compared with other existing methods such as antlion optimization algorithm, coyote optimizer, modified sine-cosine algorithm, and particle swarm optimization. Further, the power quality improvement of the network is assessed by positioning D-STATCOM, and its location is decided on the basis of the nearby bus having poor voltage profile and high total harmonic distortion (THD). The switching and controlling of D-STATCOM are assessed with fuzzy logic controller (FLC) for improving the performance parameters such as voltage profile and THD at that particular bus. The proposed analytical approach for the system is tested on the IEEE 33 bus system. It is observed that the performance of the system with the genetic algorithm gives a better solution in comparison to heuristic PDF and other existing methods for determining the optimal location and size of DG. The introduction of D-STATCOM into the system with FLC shows better performance in terms of improved voltage profile and THD in comparison to existing techniques.

Keywords: distributed generator; D-STATCOM; fuzzy logic controller; genetic algorithm; power quality



Citation: Prashant; Siddiqui, A.S.; Sarwar, M.; Althobaiti, A.; Ghoneim, S.S.M. Optimal Location and Sizing of Distributed Generators in Power System Network with Power Quality Enhancement Using Fuzzy Logic Controlled D-STATCOM. *Sustainability* **2022**, *14*, 3305. <https://doi.org/10.3390/su14063305>

Academic Editor: Mohamed A. Mohamed

Received: 4 February 2022

Accepted: 4 March 2022

Published: 11 March 2022

Publisher's Note: MDPI stays neutral with regard to jurisdictional claims in published maps and institutional affiliations.



Copyright: © 2022 by the authors. Licensee MDPI, Basel, Switzerland. This article is an open access article distributed under the terms and conditions of the Creative Commons Attribution (CC BY) license (<https://creativecommons.org/licenses/by/4.0/>).

1. Introduction

The current activities of the advanced power system have become very complicated, which needs to necessarily satisfy the increasing energy needs in an efficient manner [1,2]. The civil, fiscal, and other substantial considerations warrant the site of generation centers being placed at places distant from load centers. The reorganization and deregulation of power companies have led to making system governance unpredictable. The factors which are to be considered while carrying out extension of the transmission system are the following: cutback stability margins, chances of tripping outages, and rising power cuts. The distributed generator (DG) installation would be of the utmost benefit where the installation of new transmission lines and setting up of new power-generating units are not feasible [3–5]. It is also reasonable to believe that the selection of the right DG technology, including the optimal location and scale of the DG, would help in decreasing the losses in such a system. The purpose of optimally placing DG in a power system network is for achieving correct operation of the network with system error minimization and voltage profile enhancement inclusive of improved stability, reliability, and load

ability [6,7]. In contrast to the classical approach, smart techniques for optimal DG sizing and positioning are simple and have good convergence characteristics for application to composite power system networks [8–10]. DG is also capable of significantly mitigating harmonics and improving the voltage profile along with acquiesced transmission and distribution investment [11–13]. DG is flexible enough to locate anywhere in the system as per requirement of minimum transmission losses [14–16]. There have been many techniques proposed to perform such activities as load durability test, exact loss formula, Newton–Raphson, Gauss–Seidal method etc., [17–19]. At present, in the era of soft computing technique, every system is trying to obtain fast convergence region so as to reduce the minimum losses with lesser component involved [20,21].

The biggest challenge is to find the optimal size of DG to fulfil the load requirements. It is observed that there are four types of DG given as:

- (a) DG1: It supports only real power; no component of reactive power at unity power factor. For example: solar PV array.
- (b) DG2: It supports both real power and reactive power at 0.8–0.85 power factor leading. For example: wind, tidal geothermal.
- (c) DG3: It supports only reactive power; no component of real power at 0 power factor. For example: synchronous condenser, capacitor bank.
- (d) DG4: It absorbs the real power, giving the reactive power to the system at 0.8–0.85 power factor lagging. For example: doubly-fed induction generator [22–24].

Recent work has found that there are many advantages to the installation of DGs within the power system; namely raising the efficiency of the output and lowering energy deficit on the electrical grid [25–28]. In this article, only DG2 is used as per system requirements. The size and location of DG were proposed in many articles by using different techniques such as crow bar search method, neural network, evolutionary algorithm, intelligent water droplet, swarm optimization, etc. [29–33]. The advanced algorithms [34,35] or other existing techniques for identifying the size and location of DG have the biggest challenge of improper total harmonic distortion (THD), sensitivity, and accuracy. It is observed in literature that the THD value obtained was in the range of 15–18%, accuracy and sensitivity are also in the range of 10–15% which are quite high and inadequate, due to which voltage profile is distorted. Such issues with existing techniques create the motivation to overcome these problems. These issues are satisfactorily resolved with the proposed scheme. The genetic algorithm (GA) is proposed to determine the sizing and location of DG with improved THD, accuracy, sensitivity, and voltage profile. GA tends to be more highly permissible than heuristic optimization strategies in order to find the optimal results with less effort than absolute search. In this paper, heuristic optimization strategy which is a combination of two methods, namely, Poisson distribution method and normal distribution method, is also utilized to find the performance of the radial distribution system and show the effectiveness of GA in its comparison. Such a heuristic method requires more effort for providing detailed solutions in terms of accuracy, sensitivity, realism, and power loss. In order to have better results with minimal efforts, GA is applied. It is also observed that the proposed technique gives better results in comparison to existing techniques presented in literature [4,9,12,15,17,20,28,30,32,35–45]. However, to analyze the efficacy of the proposed work in this paper, the results achieved are compared with the existing techniques such as ant-lion optimization algorithm [42], coyote optimizer [43], modified sine-cosine algorithm [44], and particle swarm optimization [45]. The GA seems to have the main advantage of utilizing entity definition, i.e., strings, instead of handling such entities themselves. Multiple problems in electricity grid optimization are manifestations in numerical optimization but linear and other nonlinear methods in programming consider them difficult to address. In this article, the heuristic probability distribution method and GA are applied for finding the best location and sizing of DG in the IEEE 33 bus system for the constant power load model (CPLF) and the constant impedance load model (CILF). The performance parameters show the superiority of GA over the heuristic probability distribution method and other existing methods such as ant-

lion optimization algorithm [42], coyote optimizer [43], modified sine-cosine algorithm [44], and particle swarm optimization [45] in the IEEE 33 standard bus system. By considering lower real power losses, improved accuracy, and sensitivity, selection criteria of three DGs location are decided, and after that, size of DG is decided in terms of real and reactive power. Afterwards, the impact of the distribution static compensator (D-STATCOM) is assessed for improving the power quality performance at the line near to the bus terminal having higher distortion. In order to improve the power quality of performance parameters, the switching of D-STATCOM is performed by using the fuzzy logic controller (FLC). With the involvement of D-STATCOM, the distortion level has been improved considerably with FLC in comparison to existing techniques. It is preferred to utilize optimal contribution of DG for both the CILF and the CPLF system so as to fulfill the load demand using GA.

2. Optimal Location and Sizing of DG

This paper aims to find the optimal location and size of DG. For this, two approaches are adopted. Firstly, the location and size are found using the heuristic probability distribution method (PDF), and then the GA method is used. Both these methods utilize CPLF and CILF to optimize the DG location and size.

DG is placed at a particular bus to fulfil the load demand. Since load demand is fixed for all buses, the selection of bus for DG placement is assessed in terms of minimum real power losses, improved accuracy, and improved sensitivity factor. The selection of DG location is analyzed by using heuristic PDF and GA.

2.1. Heuristic Probability Distribution Method (PDF)

The location and position of DG are decided by the heuristic probability distribution method which is presented in Equation (1). The heuristic probability distribution method is a combination of the Poisson distribution method and normal distribution and it is denoted by operator 'J' and is expressed by the following equation:

$$J = \min\left(\sum_{i=1}^{33} X_i |S_i - S_{ref}|^2 + pdf(\lambda)\left(\sum_{i=1}^{33} S_{loss}\right)\right) \quad (1)$$

J is an operator of heuristic probability distribution method for minimization of power losses shown in Equation (2) and λ is the difference between measured and reference power.

$$S_{loss} = \sum_{i=1}^{33} S_i - S_{load} \quad (2)$$

S_{loss} is the complex power loss between two buses and S_{load} is the power consumed by the load.

Putting the value of Equation (2) into Equation (1), Equation (3) is obtained as:

$$J = \min\left(\sum_{i=1}^{33} X_i |S_i - S_{ref}|^2 + pdf(\lambda)\left(\sum_{i=1}^{33} S_i - S_{load}\right)\right) \quad (3)$$

where the measured (S_i) and reference value (S_{ref}) of complex power are given by Equations (4) and (5), respectively:

$$S_i = P_i + jQ_i \quad (4)$$

$$S_{ref} = P_{ref} + jQ_{ref} \quad (5)$$

X_i is the design factor given by Equation (6) to improve the accuracy such that minimum power loss can be attained.

$$X_i = \frac{S_{rated}}{|C_1 S_i + C_2 S_{ref}|^2} \quad (6)$$

The probability distribution factor in Equation (3) is given by Equation (7):

$$pdf(\lambda) = \frac{e^{-\frac{\lambda^2}{2\sigma^2}}}{\sigma\sqrt{2\pi}} \quad (7)$$

where $\lambda = S_i - S_{ref}$ = difference factor between measured and reference value of power.

As per standard expression of normal distribution and comparing with Equation (7), Equation (8) is obtained:

$$pdf(S_i - S_{ref}) = \frac{e^{-\frac{|S_i - S_{ref}|^2}{2\sigma^2}}}{\sigma\sqrt{2\pi}} \quad (8)$$

where S_{ref} is the mean, σ is the standard deviation, and its corresponding variance is given as σ^2 .

Putting the value of Equations (6)–(8) into Equation (3), Equation (9) is obtained:

$$J = \min\left(\sum_{i=1}^{33} \frac{S_{rated} |S_i - S_{ref}|^2}{|C_1 S_i + C_2 S_{ref}|^2} + \frac{e^{-\frac{|S_i - S_{ref}|^2}{2\sigma^2}}}{\sigma\sqrt{2\pi}} \left(\sum_{i=1}^{33} S_i - S_{load}\right)\right) \quad (9)$$

where,

C_1 is the accuracy measured in terms of real power measurement. Its range lies between 0.02 and 0.04. The mathematical representation of C_1 is given as $(\Delta P_i/P_i)$.

C_2 is the accuracy measured in terms of reactive power measurement. Its range lies between 0.03 and 0.05. The mathematical representation of C_2 is given as $(\Delta Q_i/Q_i)$.

Power flow at bus 'i' is given by Equations (10) and (11) as:

$$\Delta P = P_i - P_{ref} \quad (10)$$

$$\Delta Q = Q_i - Q_{ref} \quad (11)$$

where, P_i and Q_i are real and reactive power flow between two buses and their reference values are given as P_{ref} and Q_{ref} as shown in Equations (12) and (13):

$$P_i = P_{ij} = \sum_{i=1}^{33} \sum_{j=1}^{33} V_i V_j (G_{ij} \cos(\theta_i - \theta_j) + B_{ij} \sin(\theta_i - \theta_j)) \quad (12)$$

$$Q_i = Q_{ij} = \sum_{i=1}^{33} \sum_{j=1}^{33} V_i V_j (G_{ij} \sin(\theta_i - \theta_j) - B_{ij} \cos(\theta_i - \theta_j)) \quad (13)$$

where conductance (G_{ij}) and susceptance (B_{ij}) are given by Equations (14) and (15), respectively:

$$G_{ij} = \frac{R_{ij}}{\sqrt{R_{ij}^2 + X_{ij}^2}} \quad (14)$$

$$B_{ij} = \frac{X_{ij}}{\sqrt{R_{ij}^2 + X_{ij}^2}} \quad (15)$$

The best performance index can be measured by differentiating Equation (9) to obtain the minimal optimal solution as shown in Equation (16):

$$\frac{\partial J}{\partial S_i} = 0; \frac{\partial^2 J}{\partial S_i^2} > 0 \quad (16)$$

J is the function of variable S_i which employs $J(S_i)$. For checking the convergence nature, Taylor series expansion for second order is used for 'k' iteration as shown in Equation (17):

$$J(S_i^{k+1}) = J(S_i^k) + h \frac{\partial(J(S_i^k))}{\partial S_i^k} + h^2 \frac{\partial^2(J(S_i^k))}{\partial (S_i^k)^2} \quad (17)$$

Using the condition of Equation (16) in Equation (17), Equation (18) is obtained:

$$J(S_i^{k+1}) - J(S_i^k) = h^2 \frac{\partial^2(J(S_i^k))}{\partial (S_i^k)^2} \quad (18)$$

Rearranging Equation (18), Equation (19) is obtained:

$$\frac{J(S_i^{k+1}) - J(S_i^k)}{h^2} = \frac{\partial^2(J(S_i^k))}{\partial (S_i^k)^2} > 0 \quad (19)$$

where $h = S_i^{k+1} - S_i^k$. In order to obtain Equation (19), there is a constraint limit to attain the convergence level, which is shown in Equation (20):

$$\text{Magnitude} \left| J(S_i^{k+1}) - J(S_i^k) \right| < \varepsilon \quad (20)$$

The complete iterative process under the heuristic PDF method is shown using Figure 1.

The load representations for CPLF and CILF are given by Equations (21)–(23):

$$S_{load} = P_L + jQ_L \quad (21)$$

where

$$P_L = P_i \left(\frac{V_o}{V_i} \right)^x \quad (22)$$

$$Q_L = Q_i \left(\frac{V_o}{V_i} \right)^y \quad (23)$$

V_o is rated voltage of a particular bus while x and y are constant load parameter and its values are shown in Table 1.

Table 1. Constant parameter value for CPLF and CILF.

Load Type	x	y
CPLF	0	0
CILF	1.8	1.8

The constant values of x and y are taken for power load and impedance load; that is why they are called constant power load and constant impedance load.

The sensitivity and accuracy can be represented as $\frac{\partial(J)}{\partial(S_i)}$ in pu and $S_i - S_{ref}$ in pu, respectively.

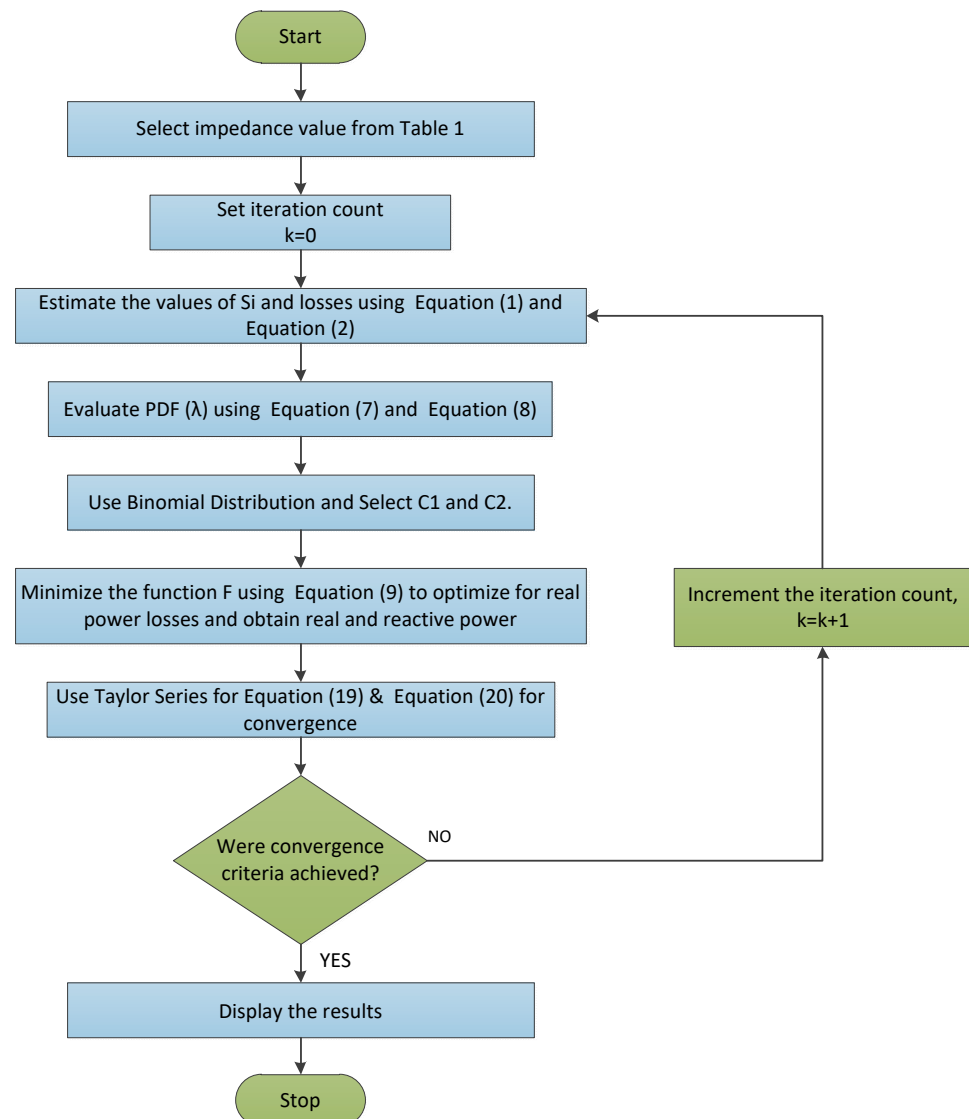


Figure 1. Flowchart of heuristic PDF method.

2.2. Performance Evaluation for Standard IEEE Tested 33 Bus Systems Using Heuristic PDF

The effectiveness of the proposed scheme using the conventional method is being tested initially on the standard IEEE 33 bus test system for CPLF and CILF [36,37]. The typical diagram of the IEEE 33 bus test system is shown in Figure 2 [37].

The IEEE 33 bus test system is modelled in MATLAB with location of fault from 0–90 km. This system consists of 33 buses and 32 lines and has 12.66 kV, 3.715 MW, and 2.3 MVar load size. Thirty percent of the entire load is the size of the source unit used. The source unit voltage is 12.66 kV and the system's lower and upper voltage is set between 0.95 pu and 1.05 pu with standard internal parameters as given in [37]. Bus 1 is considered as the slack bus or main substation. The internal parameters of the IEEE 33 bus test system are shown in [36].

The proposed design illustrated from Equations (1)–(23) is applied on the standard IEEE 33 bus test system for estimation of location of DG using the heuristic PDF method. By using these equations, the parameters such as real power loss, accuracy, and sensitivity are estimated as shown in Table 2. The design part has already been discussed in the previous section.

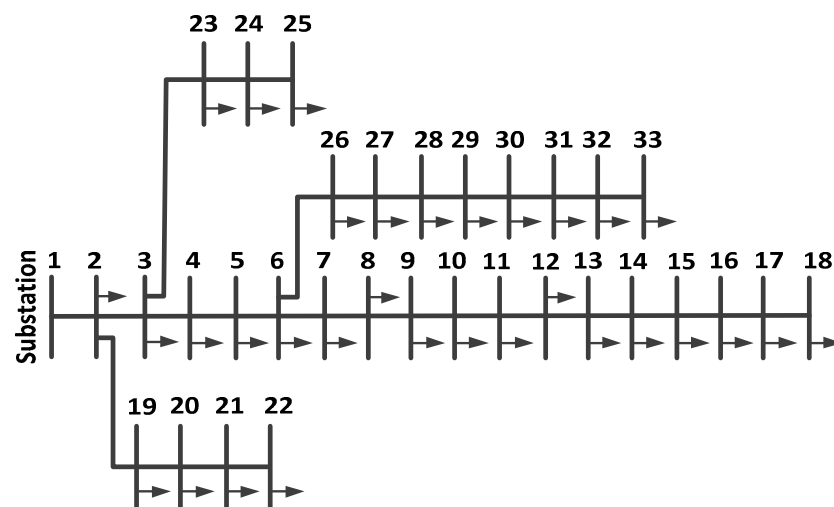


Figure 2. IEEE 33 bus test system.

Table 2. Performance parameter of DG at different locations for the IEEE 33 bus system with the heuristic PDF method for CPLF and CILF.

Bus No.	CPLF			CILF		
	Real Power Losses (pu)	Accuracy (pu)	Sensitivity (pu)	Real Power Losses (pu)	Accuracy (pu)	Sensitivity (pu)
1	0.31	0.031	0.056	0.32	0.071	0.066
2	0.29	0.029	0.047	0.31	0.087	0.065
3	0.27	0.021	0.057	0.29	0.078	0.061
4	0.21	0.019	0.056	0.30	0.079	0.055
5	0.29	0.025	0.049	0.31	0.080	0.061
6	0.28	0.031	0.054	0.27	0.079	0.059
7	0.27	0.049	0.055	0.26	0.080	0.057
8	0.31	0.050	0.061	0.25	0.090	0.056
9	0.32	0.071	0.054	0.30	0.069	0.055
10	0.31	0.072	0.049	0.31	0.091	0.053
11	0.29	0.098	0.095	0.41	0.098	0.052
12	0.31	0.098	0.075	0.29	0.084	0.049
13	0.27	0.084	0.085	0.28	0.072	0.045
14	0.29	0.087	0.084	0.31	0.073	0.044
15	0.31	0.088	0.045	0.33	0.074	0.042
16	0.27	0.086	0.039	0.32	0.078	0.043
17	0.25	0.075	0.039	0.27	0.069	0.041
18	0.27	0.069	0.042	0.29	0.081	0.048
19	0.31	0.058	0.025	0.39	0.079	0.047
20	0.30	0.047	0.024	0.40	0.081	0.046
21	0.27	0.059	0.034	0.28	0.083	0.057
22	0.29	0.098	0.036	0.31	0.087	0.051
23	0.31	0.094	0.054	0.32	0.081	0.050
24	0.27	0.095	0.045	0.33	0.079	0.065
25	0.29	0.089	0.078	0.27	0.074	0.079
26	0.27	0.075	0.084	0.31	0.072	0.065
27	0.31	0.061	0.084	0.30	0.077	0.054
28	0.33	0.072	0.094	0.32	0.076	0.051
29	0.34	0.065	0.018	0.33	0.075	0.053
30	0.35	0.050	0.045	0.31	0.091	0.064
31	0.42	0.064	0.061	0.41	0.094	0.091
32	0.41	0.042	0.082	0.43	0.080	0.085
33	0.39	0.084	0.083	0.39	0.078	0.084

2.3. Genetic Algorithm

GA is used to find the best location of DG in the IEEE 33 bus system. It involves reproduction, crossover, and mutation. Its procedure can be illustrated by the flowchart as shown in Figure 3. The process begins with selection of a binary string as shown by Equation (24), the parameters for which are assumed as follows:

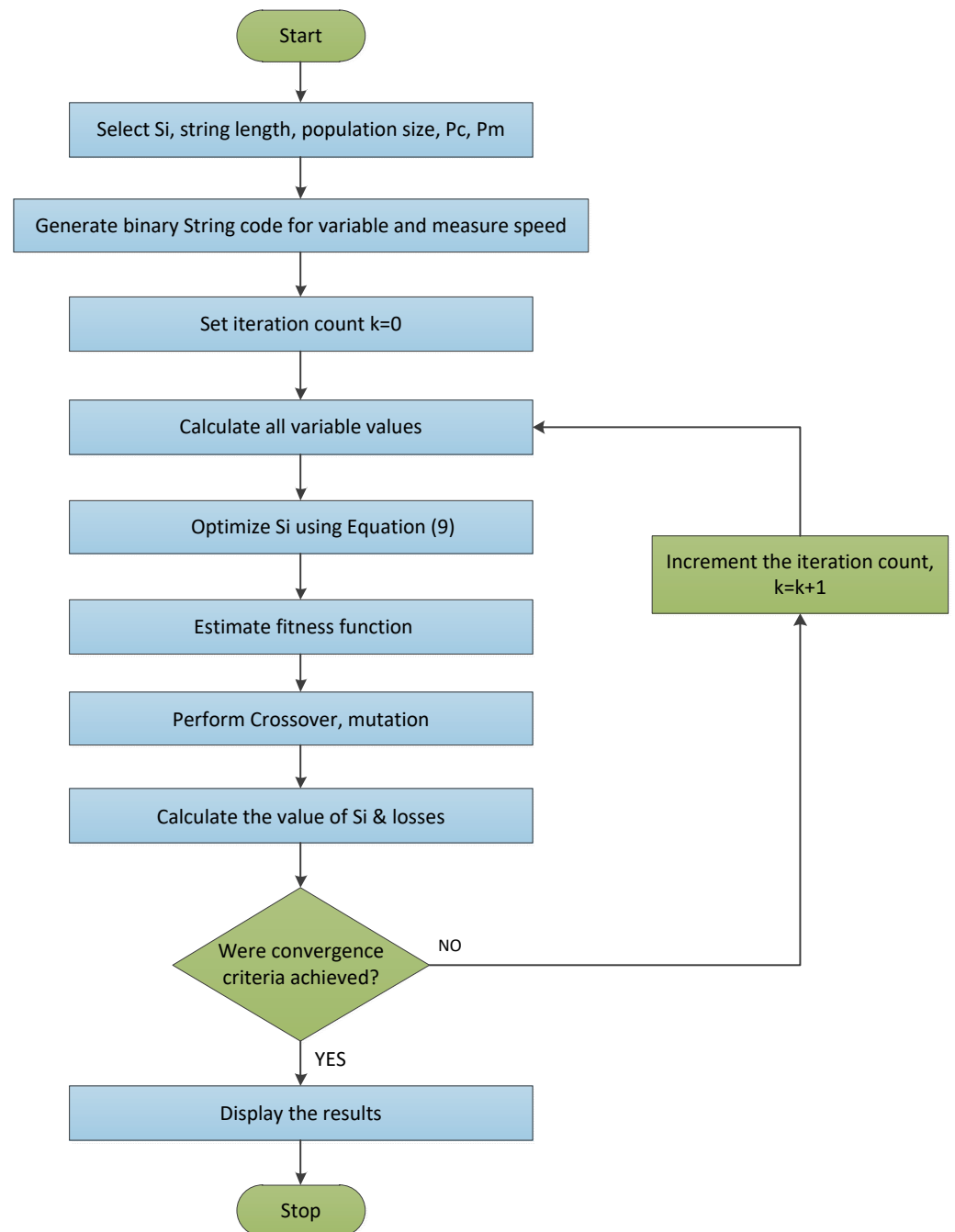


Figure 3. Flowchart representing the GA.

Population size: 6, length of the complete string: 8, crossover probability, $P_c = 0.9$, mutation probability, $P_m = 0.02$.

$$S_i^r = S_i^{\min} + \frac{S_i^{\max} - S_i^{\min}}{2^l - 1} y^r \quad (24)$$

where r is the iteration count. The application of iteration in Equation (24) results in Equations (25) and (26):

$$f^r = \frac{1}{\left(1 + \frac{\alpha \varepsilon^r}{S_i^r}\right)} \quad (25)$$

α is step size which is equal to 0.5.

$$\varepsilon^r = S_i^r - S_i^{ref} \quad (26)$$

Figures 4 and 5 show real power loss at bus 17 for CPLF and CILF using GA. The performance parameter for finding the DG location can be analyzed from Tables 2 and 3 at different DG locations in the IEEE 33 bus system using heuristic PDF and GA methods for both CPLF and CILF. Figures 6 and 7 provide the performance parameter comparison of GA with the heuristic method at different buses for CPLF and CILF. Moreover, in order to have comprehensive analysis and comparison for the DG location with GA and heuristic pdf, the results are compared with those obtained with the ant-lion optimization algorithm [42], coyote optimizer [43], modified sine-cosine algorithm [44], and particle swarm optimization [45]. The performance parameter evaluation for the estimation of DG location by using the ant-lion optimization algorithm [42], coyote optimizer [43], modified sine-cosine algorithm [44], and particle swarm optimization [45] is shown in Tables 4–7 for CPLF and CILF type of load.

From Tables 2–7, it is observed that the selection of DGs location is better found under GA for CPLF and CILF in comparison to other methods. By comparing the real power loss, sensitivity, and accuracy, it can be concluded that bus 17 is the best location for the placement of DG for both CPLF and CILF. In the sequence manner, bus 3 and bus 4 are the second and third position of placing the next two DGs. The comparative results for positioning of three DGs with different methods are shown in Table 8.

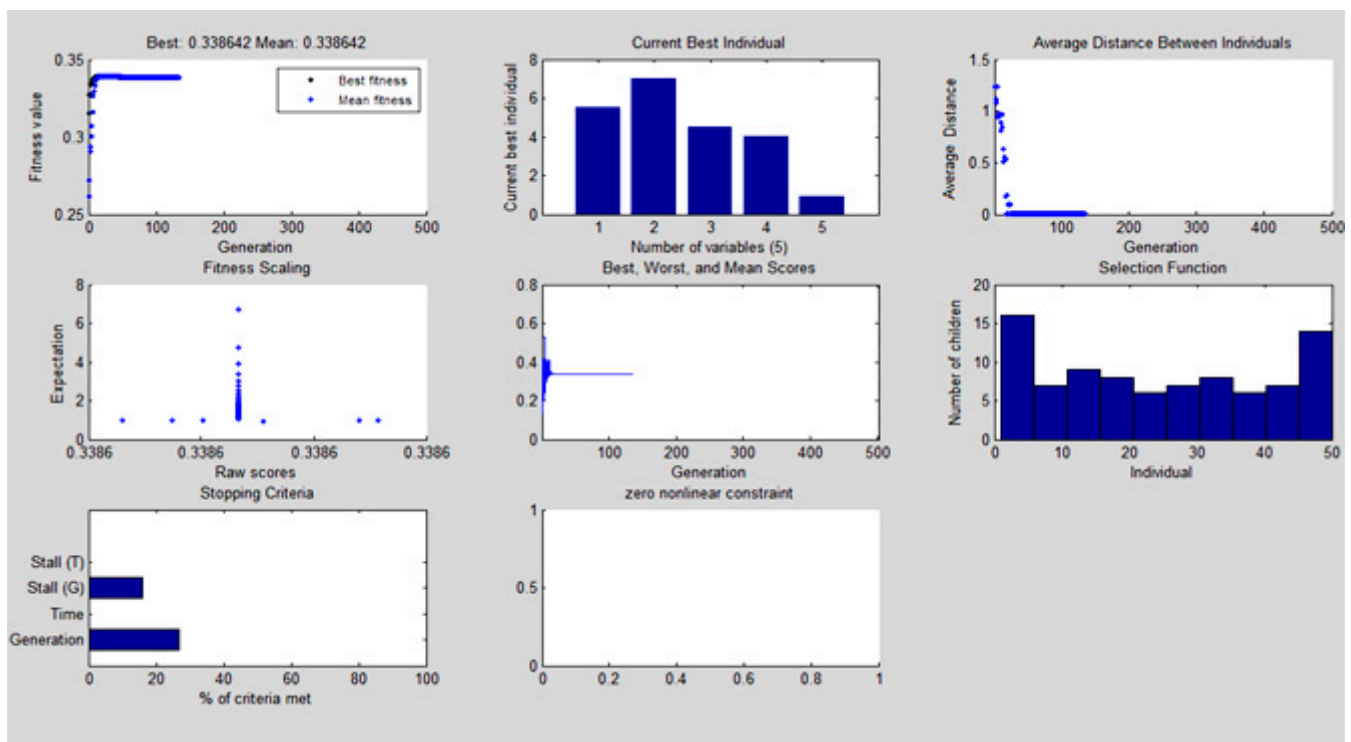


Figure 4. Real power loss at bus 17 after 150 iterations using GA for CPLF.

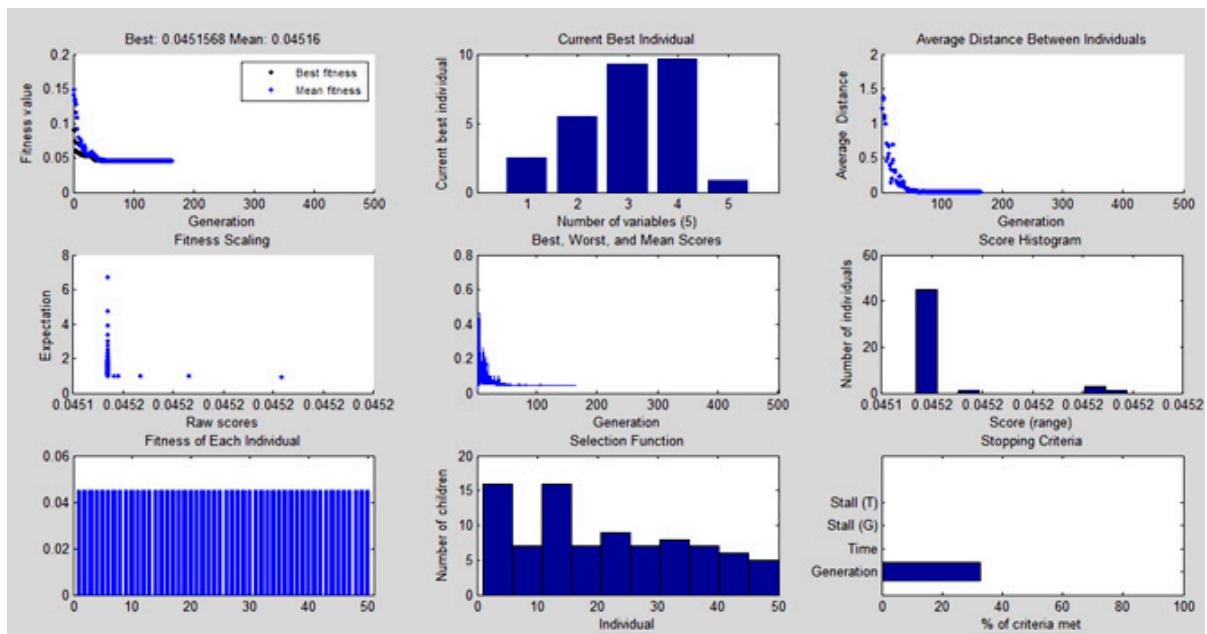


Figure 5. Real power loss at bus 17 after 155 iterations using GA for CILF.

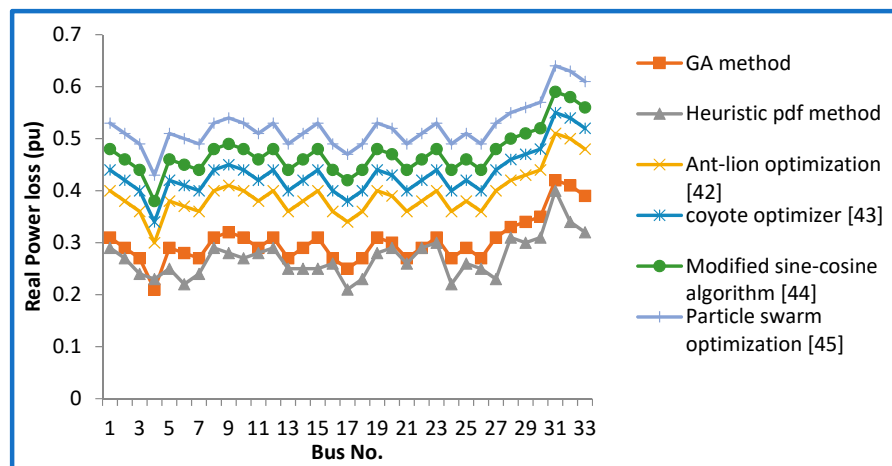


Figure 6. Real power loss comparison for CPLF.

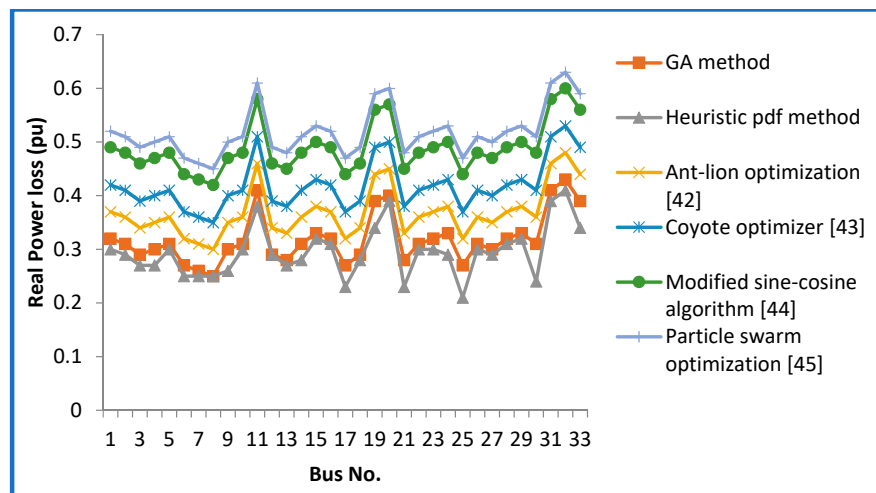


Figure 7. Real power loss comparison for CILF.

Table 3. Performance parameter of DG at different locations for the modified IEEE 33 bus system with GA for CPLF and CILF.

Bus No.	CPLF			CILF		
	Real Power Losses (pu)	Accuracy (pu)	Sensitivity (pu)	Real Power Losses (pu)	Accuracy (pu)	Sensitivity (pu)
1	0.29	0.029	0.052	0.30	0.069	0.061
2	0.27	0.027	0.044	0.29	0.082	0.059
3	0.24	0.019	0.050	0.27	0.076	0.060
4	0.23	0.017	0.051	0.27	0.078	0.052
5	0.25	0.016	0.042	0.30	0.077	0.058
6	0.22	0.024	0.051	0.25	0.078	0.055
7	0.24	0.040	0.050	0.25	0.072	0.049
8	0.29	0.045	0.052	0.25	0.084	0.051
9	0.28	0.055	0.050	0.26	0.061	0.049
10	0.27	0.056	0.048	0.30	0.089	0.050
11	0.28	0.081	0.047	0.38	0.094	0.050
12	0.29	0.089	0.069	0.29	0.082	0.045
13	0.25	0.079	0.079	0.27	0.070	0.044
14	0.25	0.079	0.078	0.28	0.071	0.043
15	0.25	0.079	0.031	0.32	0.072	0.041
16	0.26	0.076	0.037	0.31	0.075	0.041
17	0.21	0.070	0.034	0.23	0.061	0.039
18	0.23	0.065	0.032	0.28	0.070	0.041
19	0.28	0.051	0.021	0.34	0.071	0.045
20	0.29	0.045	0.022	0.39	0.072	0.041
21	0.26	0.052	0.031	0.23	0.077	0.051
22	0.29	0.091	0.035	0.30	0.081	0.047
23	0.30	0.090	0.051	0.30	0.079	0.047
24	0.22	0.091	0.044	0.29	0.071	0.047
25	0.26	0.081	0.071	0.21	0.069	0.074
26	0.25	0.070	0.081	0.30	0.069	0.064
27	0.23	0.089	0.080	0.29	0.071	0.051
28	0.31	0.090	0.079	0.31	0.072	0.049
29	0.30	0.091	0.015	0.32	0.071	0.047
30	0.31	0.081	0.035	0.24	0.085	0.059
31	0.40	0.089	0.051	0.39	0.084	0.082
32	0.34	0.081	0.073	0.41	0.077	0.071
33	0.32	0.082	0.075	0.34	0.071	0.077

Table 4. Performance parameter of DG at different locations for the IEEE 33 bus system with the ant-lion optimization algorithm [42] for CPLF and CILF.

Bus No.	CPLF			CILF		
	Real Power Losses (pu)	Accuracy (pu)	Sensitivity (pu)	Real Power Losses (pu)	Accuracy (pu)	Sensitivity (pu)
1	0.4	0.042	0.064	0.37	0.081	0.075
2	0.38	0.04	0.055	0.36	0.097	0.074
3	0.36	0.032	0.065	0.34	0.088	0.07
4	0.3	0.03	0.064	0.35	0.089	0.064
5	0.38	0.036	0.057	0.36	0.09	0.07
6	0.37	0.042	0.062	0.32	0.089	0.068
7	0.36	0.06	0.063	0.31	0.09	0.066
8	0.4	0.061	0.069	0.3	0.1	0.065
9	0.41	0.082	0.062	0.35	0.079	0.064
10	0.4	0.083	0.057	0.36	0.101	0.062
11	0.38	0.109	0.103	0.46	0.108	0.061
12	0.4	0.109	0.083	0.34	0.094	0.058
13	0.36	0.095	0.093	0.33	0.082	0.054

Table 4. Cont.

Bus No.	CPLF			CILF		
	Real Power Losses (pu)	Accuracy (pu)	Sensitivity (pu)	Real Power Losses (pu)	Accuracy (pu)	Sensitivity (pu)
14	0.38	0.098	0.092	0.36	0.083	0.053
15	0.4	0.099	0.053	0.38	0.084	0.051
16	0.36	0.097	0.047	0.37	0.088	0.052
17	0.34	0.086	0.047	0.32	0.079	0.05
18	0.36	0.08	0.05	0.34	0.091	0.057
19	0.4	0.069	0.033	0.44	0.089	0.056
20	0.39	0.058	0.032	0.45	0.091	0.055
21	0.36	0.07	0.042	0.33	0.093	0.066
22	0.38	0.109	0.044	0.36	0.097	0.06
23	0.4	0.105	0.062	0.37	0.091	0.059
24	0.36	0.106	0.053	0.38	0.089	0.074
25	0.38	0.1	0.086	0.32	0.084	0.088
26	0.36	0.086	0.092	0.36	0.082	0.074
27	0.4	0.072	0.092	0.35	0.087	0.063
28	0.42	0.083	0.102	0.37	0.086	0.06
29	0.43	0.076	0.026	0.38	0.085	0.062
30	0.44	0.061	0.053	0.36	0.101	0.073
31	0.51	0.075	0.069	0.46	0.104	0.1
32	0.5	0.053	0.09	0.48	0.09	0.094
33	0.48	0.095	0.091	0.44	0.088	0.093

Table 5. Performance parameter of DG at different locations for the IEEE 33 bus system with the coyote optimizer [43] for CPLF and CILF.

Bus No.	CPLF			CILF		
	Real Power Losses (pu)	Accuracy (pu)	Sensitivity (pu)	Real Power Losses (pu)	Accuracy (pu)	Sensitivity (pu)
1	0.44	0.051	0.068	0.42	0.088	0.082
2	0.42	0.049	0.059	0.41	0.104	0.081
3	0.4	0.041	0.069	0.39	0.095	0.077
4	0.34	0.039	0.068	0.4	0.096	0.071
5	0.42	0.045	0.061	0.41	0.097	0.077
6	0.41	0.051	0.066	0.37	0.096	0.075
7	0.4	0.069	0.067	0.36	0.097	0.073
8	0.44	0.07	0.073	0.35	0.107	0.072
9	0.45	0.091	0.066	0.4	0.086	0.071
10	0.44	0.092	0.061	0.41	0.108	0.069
11	0.42	0.118	0.107	0.51	0.115	0.068
12	0.44	0.118	0.087	0.39	0.101	0.065
13	0.4	0.104	0.097	0.38	0.089	0.061
14	0.42	0.107	0.096	0.41	0.09	0.06
15	0.44	0.108	0.057	0.43	0.091	0.058
16	0.4	0.106	0.051	0.42	0.095	0.059
17	0.38	0.095	0.051	0.37	0.086	0.057
18	0.4	0.089	0.054	0.39	0.098	0.064
19	0.44	0.078	0.037	0.49	0.096	0.063
20	0.43	0.067	0.036	0.5	0.098	0.062
21	0.4	0.079	0.046	0.38	0.1	0.073
22	0.42	0.118	0.048	0.41	0.104	0.067
23	0.44	0.114	0.066	0.42	0.098	0.066
24	0.4	0.115	0.057	0.43	0.096	0.081
25	0.42	0.109	0.09	0.37	0.091	0.095
26	0.4	0.095	0.096	0.41	0.089	0.081
27	0.44	0.081	0.096	0.4	0.094	0.07

Table 5. Cont.

Bus No.	CPLF			CILF		
	Real Power Losses (pu)	Accuracy (pu)	Sensitivity (pu)	Real Power Losses (pu)	Accuracy (pu)	Sensitivity (pu)
28	0.46	0.092	0.106	0.42	0.093	0.067
29	0.47	0.085	0.03	0.43	0.092	0.069
30	0.48	0.07	0.057	0.41	0.108	0.08
31	0.55	0.084	0.073	0.51	0.111	0.107
32	0.54	0.062	0.094	0.53	0.097	0.101
33	0.52	0.104	0.095	0.49	0.095	0.1

Table 6. Performance parameter of DG at different locations for the IEEE 33 bus system with the modified sine-cosine algorithm [44] for CPLF and CILF.

Bus No.	CPLF			CILF		
	Real Power Losses (pu)	Accuracy (pu)	Sensitivity (pu)	Real Power Losses (pu)	Accuracy (pu)	Sensitivity (pu)
1	0.48	0.059	0.075	0.49	0.096	0.089
2	0.46	0.057	0.066	0.48	0.112	0.088
3	0.44	0.049	0.076	0.46	0.103	0.084
4	0.38	0.047	0.075	0.47	0.104	0.078
5	0.46	0.053	0.068	0.48	0.105	0.084
6	0.45	0.059	0.073	0.44	0.104	0.082
7	0.44	0.077	0.074	0.43	0.105	0.08
8	0.48	0.078	0.08	0.42	0.115	0.079
9	0.49	0.099	0.073	0.47	0.094	0.078
10	0.48	0.1	0.068	0.48	0.116	0.076
11	0.46	0.126	0.114	0.58	0.123	0.075
12	0.48	0.126	0.094	0.46	0.109	0.072
13	0.44	0.112	0.104	0.45	0.097	0.068
14	0.46	0.115	0.103	0.48	0.098	0.067
15	0.48	0.116	0.064	0.5	0.099	0.065
16	0.44	0.114	0.058	0.49	0.103	0.066
17	0.42	0.103	0.058	0.44	0.094	0.064
18	0.44	0.097	0.061	0.46	0.106	0.071
19	0.48	0.086	0.044	0.56	0.104	0.07
20	0.47	0.075	0.043	0.57	0.106	0.069
21	0.44	0.087	0.053	0.45	0.108	0.08
22	0.46	0.126	0.055	0.48	0.112	0.074
23	0.48	0.122	0.073	0.49	0.106	0.073
24	0.44	0.123	0.064	0.5	0.104	0.088
25	0.46	0.117	0.097	0.44	0.099	0.102
26	0.44	0.103	0.103	0.48	0.097	0.088
27	0.48	0.089	0.103	0.47	0.102	0.077
28	0.50	0.100	0.113	0.49	0.101	0.074
29	0.51	0.093	0.037	0.50	0.1	0.076
30	0.52	0.078	0.064	0.48	0.116	0.087
31	0.59	0.092	0.08	0.58	0.119	0.114
32	0.58	0.07	0.101	0.6	0.105	0.108
33	0.56	0.112	0.102	0.56	0.103	0.107

Table 7. Performance parameter of DG at different locations for the IEEE 33 bus system with the particle swarm optimization [45] for CPLF and CILF.

Bus No.	CPLF			CILF		
	Real Power Losses (pu)	Accuracy (pu)	Sensitivity (pu)	Real Power Losses (pu)	Accuracy (pu)	Sensitivity (pu)
1	0.53	0.062	0.077	0.52	0.099	0.094
2	0.51	0.06	0.068	0.51	0.115	0.093
3	0.49	0.052	0.078	0.49	0.106	0.089
4	0.43	0.05	0.077	0.50	0.107	0.083
5	0.51	0.056	0.07	0.51	0.108	0.089
6	0.50	0.062	0.075	0.47	0.107	0.087
7	0.49	0.08	0.076	0.46	0.108	0.085
8	0.53	0.081	0.082	0.45	0.118	0.084
9	0.54	0.102	0.075	0.50	0.097	0.083
10	0.53	0.103	0.07	0.51	0.119	0.081
11	0.51	0.129	0.116	0.61	0.126	0.08
12	0.53	0.129	0.096	0.49	0.112	0.077
13	0.49	0.115	0.106	0.48	0.1	0.073
14	0.51	0.118	0.105	0.51	0.101	0.072
15	0.53	0.119	0.066	0.53	0.102	0.07
16	0.49	0.117	0.06	0.52	0.106	0.071
17	0.47	0.106	0.06	0.47	0.097	0.069
18	0.49	0.1	0.063	0.49	0.109	0.076
19	0.53	0.089	0.046	0.59	0.107	0.075
20	0.52	0.078	0.045	0.6	0.109	0.074
21	0.49	0.09	0.055	0.48	0.111	0.085
22	0.51	0.129	0.057	0.51	0.115	0.079
23	0.53	0.125	0.075	0.52	0.109	0.078
24	0.49	0.126	0.066	0.53	0.107	0.093
25	0.51	0.12	0.099	0.47	0.102	0.107
26	0.49	0.106	0.105	0.51	0.1	0.093
27	0.53	0.092	0.105	0.5	0.105	0.082
28	0.55	0.103	0.115	0.52	0.104	0.079
29	0.56	0.096	0.039	0.53	0.103	0.081
30	0.57	0.081	0.066	0.51	0.119	0.092
31	0.64	0.095	0.082	0.61	0.122	0.119
32	0.63	0.073	0.103	0.63	0.108	0.113
33	0.61	0.115	0.104	0.59	0.106	0.112

Table 8. Performance comparison among different methods.

Technique	Bus No.	CPLF			CILF		
		Real Power Loss (pu)	Accuracy (pu)	Sensitivity (pu)	Real Power Loss (pu)	Accuracy (pu)	Sensitivity (pu)
Heuristic method	17	0.25	0.075	0.039	0.27	0.069	0.041
	3	0.27	0.021	0.057	0.29	0.078	0.061
	4	0.21	0.019	0.056	0.30	0.079	0.055
Genetic Algorithm	17	0.21	0.070	0.034	0.23	0.061	0.039
	3	0.24	0.019	0.050	0.27	0.076	0.060
	4	0.23	0.017	0.051	0.27	0.078	0.052
Ant-lion optimization algorithm [42]	17	0.34	0.086	0.047	0.32	0.079	0.05
	3	0.36	0.032	0.065	0.34	0.088	0.07
	4	0.3	0.03	0.064	0.35	0.089	0.064
Coyote optimizer [43]	17	0.38	0.095	0.051	0.37	0.086	0.057
	3	0.4	0.041	0.069	0.39	0.095	0.077
	4	0.34	0.039	0.068	0.4	0.096	0.071

Table 8. Cont.

Technique	Bus No.	CPLF			CILF		
		Real Power Loss (pu)	Accuracy (pu)	Sensitivity (pu)	Real Power Loss (pu)	Accuracy (pu)	Sensitivity (pu)
Modified sine-cosine algorithm [44]	17	0.42	0.103	0.058	0.44	0.094	0.064
	3	0.44	0.049	0.076	0.46	0.103	0.084
	4	0.38	0.047	0.075	0.47	0.104	0.078
Particle Swarm optimization [45]	17	0.47	0.106	0.06	0.47	0.097	0.069
	3	0.49	0.052	0.078	0.49	0.106	0.089
	4	0.43	0.05	0.077	0.50	0.107	0.083

2.4. Optimal Sizing of DG

After deciding the optimal location of three DGs, it is also required to check the DG size to confirm its placement at bus 17. DG size is estimated from Tables 9–11 by using heuristic pdf, GA, ant-lion optimization algorithm [42], coyote optimizer [43], modified sine-cosine algorithm [44], and particle swarm optimization [45] for both CPLF and CILF type of load. It is observed that the size of DG when placed at bus 17 is found to be the minimum. The relative comparison of DG size for bus 17, 4, and 3 is shown in Table 12. The minimal size of DG is obtained under GA as compared to the heuristic method. Figures 8–10 illustrate the real power and Figure 11 illustrates the reactive power at bus 17 for both CPLF and CILF. From the results, it is confirmed that bus 17 is the best choice for the location and optimum sizing of DG is also obtained here. Subsequently, bus 3 and bus 4 have the appropriate size of DGs, which assures the confirmation of the DG location. The location and size of three DGs at the allotted location in the IEEE 33 bus system are shown in Figure 12.

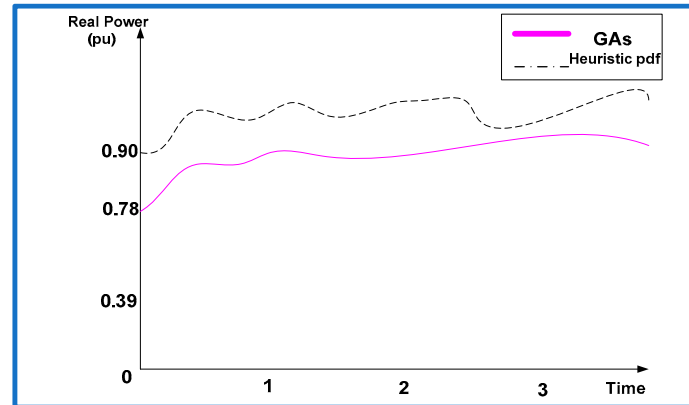


Figure 8. Real power at bus 17 after 150 iterations for CPLF.

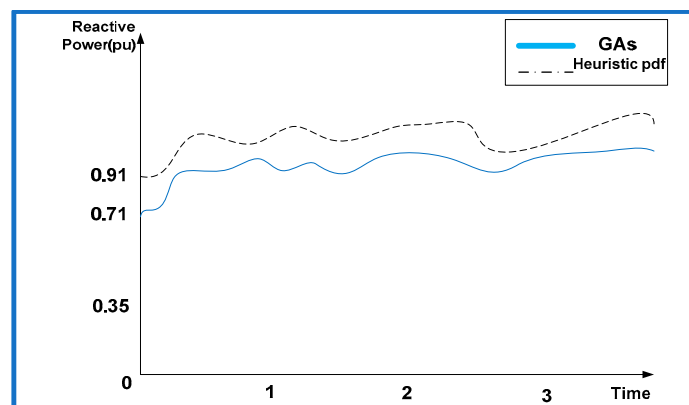


Figure 9. Reactive power at bus 17 after 150 iterations using GA for CPLF.

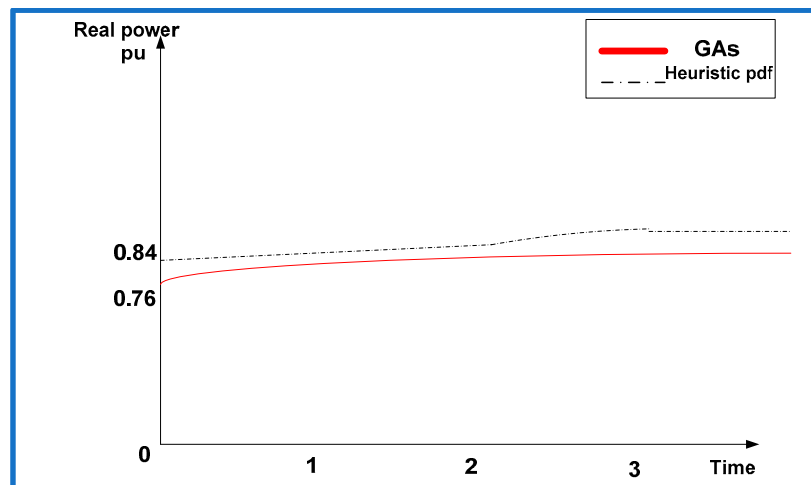


Figure 10. Real power at bus 17 after 155 iterations using GA for CILF.

Table 9. DG size comparison for CPLF and CILF using GA and heuristic PDF.

Bus No.	CPLF				CILF			
	Heuristic PDF		GA		Heuristic PDF		GA	
	P (pu)	Q (pu)	P (pu)	Q (pu)	P (pu)	Q (pu)	P (pu)	Q (pu)
1	1.01	0.98	1.02	0.99	1.09	1.02	0.99	1.02
2	1.02	0.94	1.10	0.96	1.03	0.99	1.01	0.99
3	1.05	0.85	0.85	0.78	1.10	1.01	0.90	0.89
4	1.23	0.99	0.91	0.81	1.09	0.95	0.81	0.91
5	1.12	1.01	1.31	0.75	1.11	0.99	1.29	0.76
6	1.03	0.94	1.05	0.73	1.05	1.02	1.01	0.85
7	1.04	0.96	1.06	0.74	1.07	0.95	1.10	0.72
8	0.91	0.95	0.95	0.91	1.02	0.97	0.99	0.84
9	0.89	0.81	0.97	0.82	0.95	0.95	0.94	0.92
10	1.02	0.95	1.03	0.76	0.98	0.92	1.01	0.96
11	0.99	1.00	0.99	1.02	1.02	1.05	0.98	1.01
12	0.98	1.01	0.99	1.03	0.99	1.03	0.92	1.01
13	1.89	1.03	1.95	1.04	1.71	1.02	1.84	1.00
14	0.85	1.05	0.85	1.05	0.97	1.05	1.12	1.01
15	0.94	1.09	0.94	1.10	1.00	0.99	0.99	1.10
16	0.94	1.11	0.98	1.01	0.99	1.02	0.94	1.08
17	0.89	0.90	0.78	0.71	0.84	0.98	0.76	0.70
18	0.95	1.13	0.96	1.04	1.05	1.10	0.99	1.01
19	0.94	1.84	0.99	1.88	0.92	1.21	0.94	1.08
20	1.00	1.24	1.07	1.44	1.10	1.12	1.02	1.40
21	1.00	1.11	1.08	1.21	1.09	1.01	1.02	1.01
22	0.95	1.24	1.98	1.34	1.01	1.10	1.91	1.21
23	0.80	1.00	1.89	1.44	1.02	1.08	1.21	1.01
24	0.81	0.99	1.85	1.00	0.95	1.01	1.01	1.09
25	0.79	1.20	1.84	1.22	0.89	1.12	1.00	1.12
26	0.84	1.21	1.85	1.23	0.94	1.12	1.02	1.11
27	0.99	0.99	2.00	1.02	0.96	0.96	1.01	1.10
28	0.98	0.84	1.75	0.86	1.03	1.01	1.05	0.95
29	0.99	0.95	1.82	0.98	1.21	0.99	1.51	0.97
30	1.33	0.99	1.72	0.99	1.23	0.92	1.10	0.94
31	0.99	1.00	1.81	1.01	1.42	1.01	1.02	1.08
32	1.20	1.01	1.51	1.05	1.47	1.11	1.01	1.06
33	1.05	1.12	1.31	1.15	1.25	1.10	1.01	1.01

Table 10. DG size comparison for CPLF and CILF using the ant-lion optimization algorithm [42] and coyote optimizer [43].

Bus No.	CPLF				CILF			
	Ant-Lion Optimization Algorithm [42]		Coyote Optimizer [43]		Ant-Lion Optimization Algorithm [42]		Coyote Optimizer [43]	
	P (pu)	Q (pu)	P (pu)	Q (pu)	P (pu)	Q (pu)	P (pu)	Q (pu)
1	1.1	1.04	1.08	1.07	1.18	1.11	1.07	1.09
2	1.11	1	1.16	1.04	1.12	1.08	1.09	1.06
3	1.14	0.91	0.91	0.86	1.19	1.1	0.98	0.96
4	1.32	1.05	0.97	0.89	1.18	1.04	0.89	0.98
5	1.21	1.07	1.37	0.83	1.2	1.08	1.37	0.83
6	1.12	1	1.11	0.81	1.14	1.11	1.09	0.92
7	1.13	1.02	1.12	0.82	1.16	1.04	1.18	0.79
8	1	1.01	1.01	0.99	1.11	1.06	1.07	0.91
9	0.98	0.87	1.03	0.9	1.04	1.04	1.02	0.99
10	1.11	1.01	1.09	0.84	1.07	1.01	1.09	1.03
11	1.08	1.06	1.05	1.1	1.11	1.14	1.06	1.08
12	1.07	1.07	1.05	1.11	1.08	1.12	1	1.08
13	1.98	1.09	2.01	1.12	1.8	1.11	1.92	1.07
14	0.94	1.11	0.91	1.13	1.06	1.14	1.2	1.08
15	1.03	1.15	1	1.18	1.09	1.08	1.07	1.17
16	1.03	1.17	1.04	1.09	1.08	1.11	1.02	1.15
17	0.98	0.96	0.84	0.79	0.93	1.07	0.84	0.77
18	1.04	1.19	1.02	1.12	1.14	1.19	1.07	1.08
19	1.03	1.9	1.05	1.96	1.01	1.3	1.02	1.15
20	1.09	1.3	1.13	1.52	1.19	1.21	1.1	1.47
21	1.09	1.17	1.14	1.29	1.18	1.1	1.1	1.08
22	1.04	1.3	2.04	1.42	1.1	1.19	1.99	1.28
23	0.89	1.06	1.95	1.52	1.11	1.17	1.29	1.08
24	0.9	1.05	1.91	1.08	1.04	1.1	1.09	1.16
25	0.88	1.26	1.9	1.3	0.98	1.21	1.08	1.19
26	0.93	1.27	1.91	1.31	1.03	1.21	1.1	1.18
27	1.08	1.05	2.06	1.1	1.05	1.05	1.09	1.17
28	1.07	0.9	1.81	0.94	1.12	1.1	1.13	1.02
29	1.08	1.01	1.88	1.06	1.3	1.08	1.59	1.04
30	1.42	1.05	1.78	1.07	1.32	1.01	1.18	1.01
31	1.08	1.06	1.87	1.09	1.51	1.1	1.1	1.15
32	1.29	1.07	1.57	1.13	1.56	1.2	1.09	1.13
33	1.14	1.18	1.37	1.23	1.34	1.19	1.09	1.08

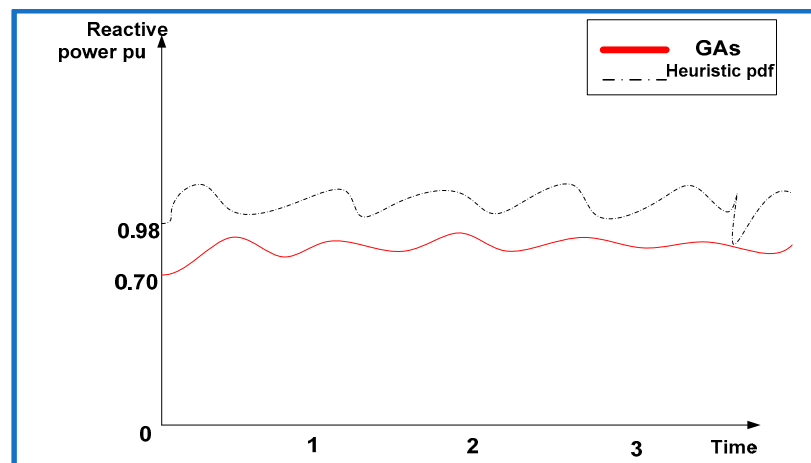


Figure 11. Reactive power at bus 17 after 155 iterations using GA for CILF.

Table 11. DG size comparison for CPLF and CILF using the modified sine-cosine algorithm [44] and particle swarm optimization [45].

Bus No.	CPLF				CILF			
	Modified Sine-Cosine Algorithm [44]		Particle Swarm Optimization [45]		Modified Sine-Cosine Algorithm [44]		Particle Swarm Optimization [45]	
	P (pu)	Q (pu)	P (pu)	Q (pu)	P (pu)	Q (pu)	P (pu)	Q (pu)
1	1.19	1.1	1.14	1.15	1.27	1.2	1.15	1.16
2	1.2	1.06	1.22	1.12	1.21	1.17	1.17	1.13
3	1.23	0.97	0.97	0.94	1.28	1.19	1.06	1.03
4	1.41	1.11	1.03	0.97	1.27	1.13	0.97	1.05
5	1.3	1.13	1.43	0.91	1.29	1.17	1.45	0.9
6	1.21	1.06	1.17	0.89	1.23	1.2	1.17	0.99
7	1.22	1.08	1.18	0.9	1.25	1.13	1.26	0.86
8	1.09	1.07	1.07	1.07	1.2	1.15	1.15	0.98
9	1.07	0.93	1.09	0.98	1.13	1.13	1.1	1.06
10	1.2	1.07	1.15	0.92	1.16	1.1	1.17	1.1
11	1.17	1.12	1.11	1.18	1.2	1.23	1.14	1.15
12	1.16	1.13	1.11	1.19	1.17	1.21	1.08	1.15
13	2.07	1.15	2.07	1.2	1.89	1.2	2	1.14
14	1.03	1.17	0.97	1.21	1.15	1.23	1.28	1.15
15	1.12	1.21	1.06	1.26	1.18	1.17	1.15	1.24
16	1.12	1.23	1.1	1.17	1.17	1.2	1.1	1.22
17	1.07	1.02	0.9	0.87	1.02	1.16	0.92	0.84
18	1.13	1.25	1.08	1.2	1.23	1.28	1.15	1.15
19	1.12	1.96	1.11	2.04	1.1	1.39	1.1	1.22
20	1.18	1.36	1.19	1.6	1.28	1.3	1.18	1.54
21	1.18	1.23	1.2	1.37	1.27	1.19	1.18	1.15
22	1.13	1.36	2.1	1.5	1.19	1.28	2.07	1.35
23	0.98	1.12	2.01	1.6	1.2	1.26	1.37	1.15
24	0.99	1.11	1.97	1.16	1.13	1.19	1.17	1.23
25	0.97	1.32	1.96	1.38	1.07	1.3	1.16	1.26
26	1.02	1.33	1.97	1.39	1.12	1.3	1.18	1.25
27	1.17	1.11	2.12	1.18	1.14	1.14	1.17	1.24
28	1.16	0.96	1.87	1.02	1.21	1.19	1.21	1.09
29	1.17	1.07	1.94	1.14	1.39	1.17	1.67	1.11
30	1.51	1.11	1.84	1.15	1.41	1.1	1.26	1.08
31	1.17	1.12	1.93	1.17	1.6	1.19	1.18	1.22
32	1.38	1.13	1.63	1.21	1.65	1.29	1.17	1.2
33	1.23	1.24	1.43	1.31	1.43	1.28	1.17	1.15

Table 12. DG size comparison at the three best bus locations.

Load Type	Bus No.	Heuristic Method		Genetic Algorithm		Ant-Lion Optimization Algorithm [42]		Coyote Optimizer [43]		Modified Sine-Cosine Algorithm [44]		Particle Swarm Optimization [45]	
		P (pu)	Q (pu)	P (pu)	Q (pu)	P (pu)	Q (pu)	P (pu)	Q (pu)	P (pu)	Q (pu)	P (pu)	Q (pu)
CPLF	17	0.89	0.9	0.78	0.71	0.98	0.96	0.84	0.79	0.98	0.96	0.84	0.79
CILF		0.84	0.98	0.76	0.7	0.93	1.07	0.84	0.77	0.93	1.07	0.84	0.77
CPLF	3	1.05	0.85	0.85	0.78	1.14	0.91	0.91	0.86	1.14	0.91	0.91	0.86
CILF		1.1	1.01	0.9	0.89	1.19	1.1	0.98	0.96	1.19	1.1	0.98	0.96
CPLF	4	1.23	0.99	0.91	0.81	1.32	1.05	0.97	0.89	1.32	1.05	0.97	0.89
CILF		1.09	0.95	0.81	0.91	1.18	1.04	0.89	0.98	1.18	1.04	0.89	0.98

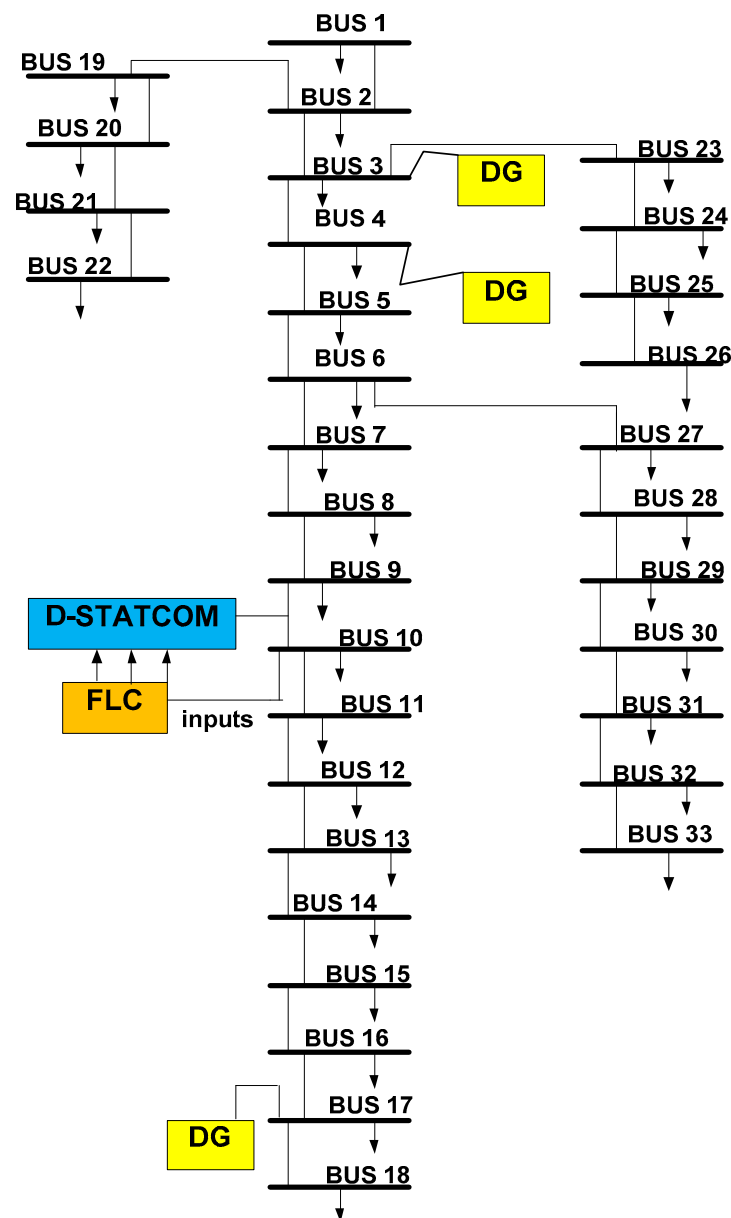


Figure 12. Layout of the IEEE 33 bus system with allocated positioning and sizing of DG and D-STATCOM.

3. Positioning and Impact of D-STATCOM

The positioning and impact of D-STATCOM in the IEEE-33 bus system have to be assessed for improving the power quality performance parameters such as THD and voltage profile. The rating of D-STATCOM is 1 pu reactive power. In order to improve power quality performance, control of D-STATCOM is decided by using the fuzzy logic controller. In this article, only one D-STATCOM is used, so it has to be connected at that bus where large distortions are present. In order to define the inputs and output of FLC, Equation (9) is further used. Now, we differentiate Equation (9) to obtain the optimal solution.

$$\text{Let's define } E = S_i - S_{ref} \quad (27)$$

$$\frac{d(J)}{dE} = 0 \quad (28)$$

Equation (27) enables us to differentiate J with respect to E as given in Equation (28). After differentiating, Equation (29) is obtained:

$$e^{-\frac{|E|^2}{2\sigma^2}} = \frac{S_{rated}\sigma\sqrt{2\pi}}{|C_1S_i + C_2S_{ref}|2(S_i - S_{load})} \quad (29)$$

By arranging the terms in Equation (29) and by taking log on both sides, the value of E is obtained as given by Equation (30).

$$E = \sqrt{2\sigma^2 \log\left(\frac{|C_1S_i + C_2S_{ref}|2(S_i - S_{load})}{|S_{rated}\sigma\sqrt{2\pi}|}\right)} \quad (30)$$

Equation (30) gives the optimal solution. Now, the inputs to FLC are error (E) and change in error (ΔE) which are shown in Equation (31) as:

$$\Delta E = E(t) - E(t - 1) \quad (31)$$

The detailed structure of the D-STATCOM-based FLC controller is shown in Figures 13 and 14. In Figure 13, distorted real and reactive power is measured and passes through the PID controller which generates the measured complex power. The measured complex power is compared with its reference value which produces error. The error and derivative of error act as inputs to FLC. The actual design of FLC for D-STATCOM switching is shown in Figure 14. The output of FLC is reference voltage which is compared with reference value and generates pulses for switching the D-STATCOM. In the same pattern, ΔE can be expressed in standard form.

In order to design rules of the fuzzy set, a 7×7 matrix is taken so that the model will have more precise and better results. This means both inputs have seven membership functions. Using Cramer's product rule, FLC rule is designed as shown in Figure 15 and its surface view is shown in Figure 16. Tables 13 and 14 show the notification of membership function for first input, as initial error E is around 0.12 and mapping of input with output, respectively.

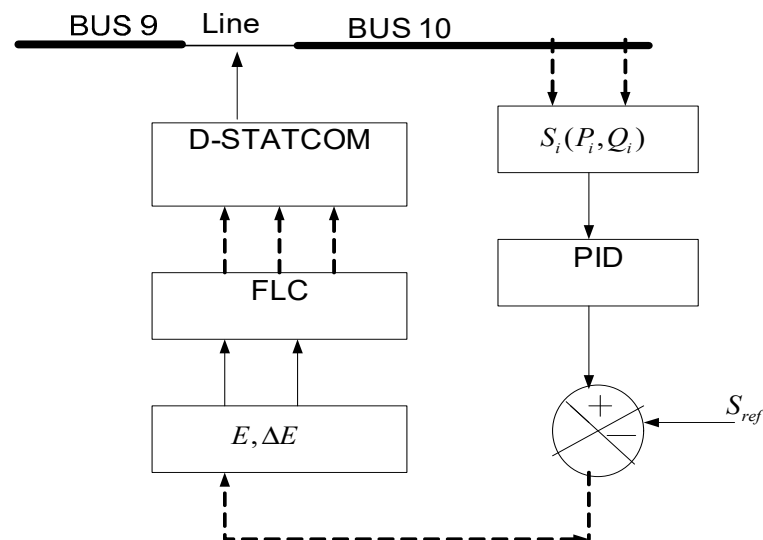


Figure 13. Structure of D-STATCOM-based FLC controller.

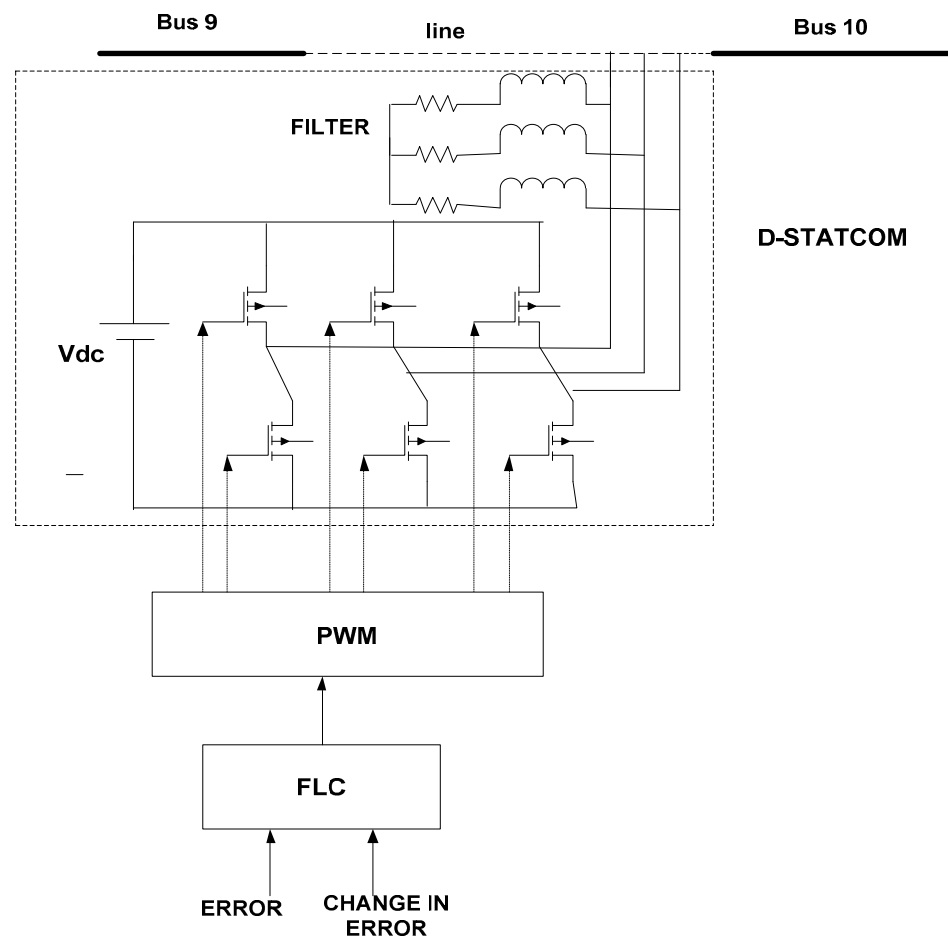


Figure 14. Switching of D-STATCOM.

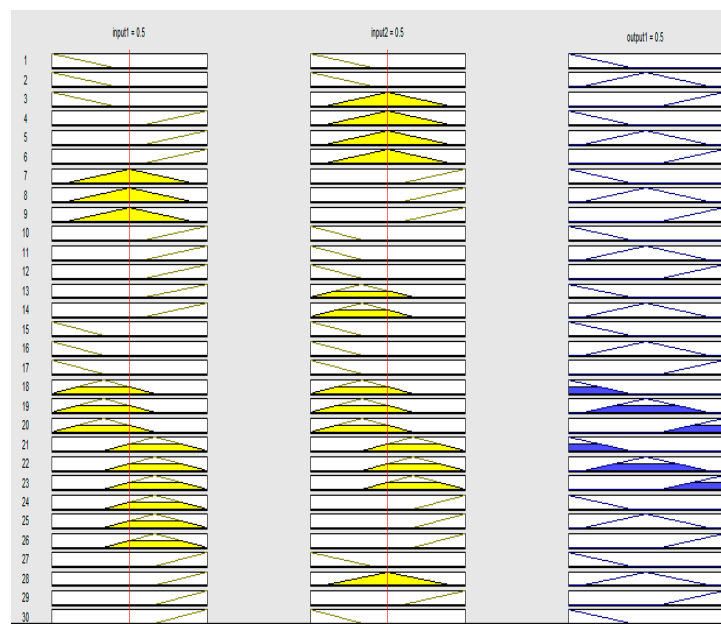


Figure 15. Fuzzy rules of FLC.

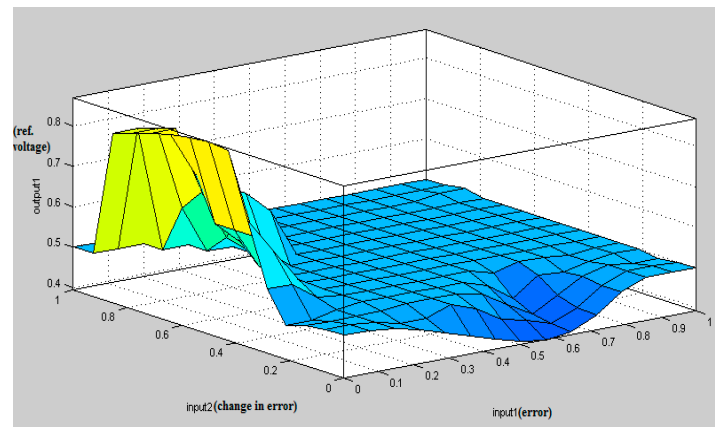


Figure 16. Surface view of FLC between inputs and output.

Table 13. Mathematical notation of input and output.

$E/\Delta E$		NB	NM	NS	ZS	PS	PM	PB
		0.15	0.40	0.65	0.9	0.65	0.40	0.15
NB	0.25	0.25	0.40	0.65	0.9	0.65	0.40	0.25
NM	0.50	0.50	0.50	0.65	0.9	0.65	0.50	0.50
NS	0.75	0.75	0.75	0.75	0.9	0.75	0.75	0.75
ZS	1	1	1	1	1	1	1	1
PS	0.75	0.75	0.75	0.75	0.9	0.75	0.75	0.75
PM	0.50	0.50	0.50	0.65	0.9	0.65	0.50	0.50
PB	0.25	0.25	0.40	0.65	0.9	0.65	0.40	0.25

Table 14. Mapping of output with input.

$E/\Delta E$	NB	NM	NS	ZS	PS	PM	PB
NB	NM	NS	ZS	PS	PM	PB	PM
NB	NB	NM	NS	ZS	PS	PM	PB
NM	NM	NM	NS	ZS	PS	NM	NM
NS	NS	NS	NS	ZS	NS	NS	NS
ZS	ZS	ZS	ZS	ZS	ZS	ZS	ZS
PS	PS	PS	PS	ZS	PS	PS	PS
PM	PM	PM	NS	ZS	PS	PM	PM

From Tables 13 and 14, it can be demonstrated that, under certain parameters, a precise control of objectives can be achieved using fuzzy observations, mapping, and control, if the observations become sufficiently accurate as the goal is approached.

The seven membership functions corresponding to the first input are shown in Equation (32) and these seven membership functions are taken from x_1 to x_7 . The seven membership functions are chosen in order to have better and more precise results. The nature of the membership function is triangular and input is split into seven membership functions. Each membership function from x_1 to x_7 is assigned with values in the numerator as shown in Equation (32).

$$E = \frac{0.03}{x_1} + \frac{0.06}{x_2} + \frac{0.09}{x_3} + \frac{0.12}{x_4} + \frac{0.09}{x_5} + \frac{0.06}{x_6} + \frac{0.03}{x_7} \tag{32}$$

Dividing Equation (32) by 0.12, Equation (33) is obtained as:

$$E = \frac{0.25}{x_1} + \frac{0.50}{x_2} + \frac{0.75}{x_3} + \frac{1}{x_4} + \frac{0.75}{x_5} + \frac{0.50}{x_6} + \frac{0.25}{x_7} \tag{33}$$

Notification of membership function for the second input is given in Equation (34):

$$\Delta E = \frac{0.15}{x_1} + \frac{0.40}{x_2} + \frac{0.65}{x_3} + \frac{0.9}{x_4} + \frac{0.65}{x_5} + \frac{0.40}{x_6} + \frac{0.15}{x_7} \quad (34)$$

From the Cartesian product rule:

$$A = EB = \Delta E, A \cup B = \max(A \text{ or } B)$$

Further membership function is taken as:

$$x_1 = NB, x_2 = NM, x_3 = NS, x_4 = ZS, x_5 = PS, x_6 = PM, x_7 = PB$$

Table 15 gives the comparative analysis of voltage profile at different buses with different existing techniques and D-STATCOM-based FLC for both CPLF and CILF load; whereas computational expression of THD is given by Equation (35).

Table 16 gives the comparative analysis of THD (%) of real power different buses with different existing techniques and D-STATCOM-based FLC for both CPLF and CILF load.

$$THD = \sqrt{\frac{1}{g^2} - 1} \quad (35)$$

where 'g' is distortion factor which is defined as ratio of rms fundamental harmonic value to rms value of voltage.

Table 15. Voltage (pu) comparisons at different buses with D-STATCOM-based FLC and existing methods.

Bus No.	Load Type	D-STATCOM-Based FLC	Harmony Search Algorithm [4]	Ant Colony Algorithm [9]	Big-Bang-Crunch Method [30]
1	CPLF	0.86	0.81	0.78	0.74
	CILF	0.87	0.82	0.79	0.75
2	CPLF	0.86	0.81	0.78	0.74
	CILF	0.85	0.8	0.79	0.75
3	CPLF	0.87	0.82	0.81	0.77
	CILF	0.86	0.81	0.8	0.76
4	CPLF	0.85	0.8	0.78	0.74
	CILF	0.87	0.82	0.8	0.76
5	CPLF	0.86	0.81	0.77	0.73
	CILF	0.85	0.8	0.79	0.75
6	CPLF	0.85	0.8	0.79	0.75
	CILF	0.9	0.85	0.83	0.79
7	CPLF	0.9	0.85	0.83	0.79
	CILF	0.91	0.86	0.84	0.8
8	CPLF	0.91	0.86	0.83	0.79
	CILF	0.91	0.86	0.82	0.78
9	CPLF	0.91	0.86	0.84	0.8
	CILF	0.91	0.86	0.84	0.8
10	CPLF	1	0.98	0.97	0.93
	CILF	1.01	0.99	0.97	0.93
11	CPLF	0.9	0.85	0.82	0.78
	CILF	0.92	0.87	0.85	0.81
12	CPLF	0.76	0.71	0.87	0.83
	CILF	0.79	0.74	0.72	0.68

Table 15. Cont.

Bus No.	Load Type	D-STATCOM-Based FLC	Harmony Search Algorithm [4]	Ant Colony Algorithm [9]	Big-Bang-Crunch Method [30]
13	CPLF	0.8	0.75	0.73	0.69
	CILF	0.81	0.76	0.74	0.7
14	CPLF	0.79	0.74	0.72	0.68
	CILF	0.8	0.75	0.74	0.7
15	CPLF	0.8	0.75	0.73	0.69
	CILF	0.74	0.69	0.65	0.61
16	CPLF	0.89	0.84	0.81	0.77
	CILF	0.9	0.85	0.83	0.79
17	CPLF	0.99	0.97	0.94	0.9
	CILF	0.98	0.95	0.9	0.86
18	CPLF	0.95	0.9	0.89	0.85
	CILF	0.93	0.88	0.86	0.81
19	CPLF	0.97	0.92	0.91	0.87
	CILF	0.95	0.9	0.87	0.83
20	CPLF	0.96	0.91	0.89	0.85
	CILF	0.9	0.85	0.83	0.79
21	CPLF	0.91	0.86	0.84	0.8
	CILF	0.93	0.88	0.81	0.77
22	CPLF	0.94	0.89	0.84	0.8
	CILF	0.76	0.71	0.7	0.66
23	CPLF	0.75	0.7	0.69	0.65
	CILF	0.74	0.69	0.68	0.64
24	CPLF	0.73	0.68	0.67	0.63
	CILF	0.72	0.67	0.66	0.62
25	CPLF	0.71	0.66	0.64	0.6
	CILF	0.7	0.65	0.64	0.6
26	CPLF	0.71	0.66	0.64	0.6
	CILF	0.69	0.64	0.63	0.59
27	CPLF	0.7	0.65	0.62	0.58
	CILF	0.71	0.66	0.64	0.6
28	CPLF	0.72	0.67	0.65	0.61
	CILF	0.72	0.67	0.64	0.6
29	CPLF	0.72	0.67	0.65	0.61
	CILF	0.75	0.7	0.69	0.65
30	CPLF	0.76	0.71	0.7	0.66
	CILF	0.76	0.71	0.7	0.66
31	CPLF	0.81	0.76	0.74	0.7
	CILF	0.77	0.72	0.71	0.67
32	CPLF	0.78	0.73	0.72	0.68
	CILF	0.79	0.74	0.73	0.69
33	CPLF	0.8	0.75	0.74	0.7
	CILF	0.78	0.73	0.72	0.68

Table 16. THD (%) of real power comparison at different buses with D-STATCOM-based FLC and existing methods.

Bus No.	Load Type	D-STATCOM-Based FLC	Harmony Search Algorithm [4]	Ant Colony Algorithm [9]	Big-Bang–Crunch Method [30]
1	CPLF	6.81	7.81	8.21	8.82
	CILF	6.82	7.82	7.91	8.52
2	CPLF	7.81	8.81	9.12	9.73
	CILF	6.8	7.8	7.91	8.52
3	CPLF	7.71	8.71	9.11	9.72
	CILF	6.81	7.81	8.81	9.42
4	CPLF	6.8	7.8	9.11	9.72
	CILF	6.82	7.82	8.11	8.72
5	CPLF	6.81	7.81	8.1	8.71
	CILF	8.9	9.9	9.21	9.82
6	CPLF	6.8	7.8	9.17	9.78
	CILF	8.5	8.5	9.12	9.73
7	CPLF	8.4	8.4	9.14	9.75
	CILF	6.86	7.86	8.98	9.59
8	CPLF	6.86	7.86	9.12	9.73
	CILF	6.86	7.86	8.65	9.26
9	CPLF	7.5	8.5	8.88	9.49
	CILF	7.4	8.4	8.78	9.39
10	CPLF	5.2	9.12	9.89	10.5
	CILF	6.3	9.65	9.65	10.26
11	CPLF	7.6	8.6	8.89	9.5
	CILF	7.5	8.5	8.92	9.53
12	CPLF	6.71	7.71	7.87	8.48
	CILF	7.1	8.1	8.55	9.16
13	CPLF	7.6	8.6	8.77	9.38
	CILF	7.7	8.7	8.88	9.49
14	CPLF	7.1	8.1	8.9	9.51
	CILF	7.5	8.5	8.87	9.48
15	CPLF	6.75	7.75	7.87	8.48
	CILF	6.69	7.69	7.99	8.6
16	CPLF	6.84	7.84	7.98	8.59
	CILF	6.85	7.85	8.02	8.63
17	CPLF	6.2	7.25	9.02	9.63
	CILF	7.3	7.95	8.22	8.83
18	CPLF	6.9	7.9	7.99	8.6
	CILF	6.91	7.91	7.95	8.56
19	CPLF	6.92	7.92	8.25	8.86
	CILF	6.9	7.9	8.65	9.26
20	CPLF	6.91	7.91	8.14	8.75
	CILF	6.85	7.85	9.02	9.63
21	CPLF	6.86	7.86	9.22	9.83
	CILF	6.88	7.88	8.99	9.6
22	CPLF	6.89	7.89	8.55	9.16
	CILF	6.71	7.71	8.42	9.03
23	CPLF	6.7	7.7	8.11	8.72
	CILF	6.69	7.69	7.87	8.48

Table 16. Cont.

Bus No.	Load Type	D-STATCOM-Based FLC	Harmony Search Algorithm [4]	Ant Colony Algorithm [9]	Big-Bang–Crunch Method [30]
24	CPLF	6.68	7.68	7.98	8.59
	CILF	6.67	7.67	7.84	8.45
25	CPLF	6.66	7.66	7.92	8.53
	CILF	6.65	7.65	7.83	8.44
26	CPLF	6.66	7.66	7.8	8.41
	CILF	6.64	7.64	7.75	8.36
27	CPLF	6.65	7.65	7.79	8.4
	CILF	6.66	7.66	7.85	8.46
28	CPLF	6.67	7.67	7.87	8.48
	CILF	6.67	7.67	7.9	8.51
29	CPLF	6.67	7.67	7.75	8.36
	CILF	6.7	7.7	7.98	8.59
30	CPLF	6.69	7.69	7.87	8.48
	CILF	6.61	7.61	7.9	8.51
31	CPLF	6.66	7.66	7.96	8.57
	CILF	6.72	7.72	7.92	8.53
32	CPLF	6.73	7.73	7.93	8.54
	CILF	6.65	7.65	7.95	8.56
33	CPLF	6.5	7.5	7.84	8.45
	CILF	6.73	7.73	7.83	8.44

Now, a suitable location for D-STATCOM at a particular bus has to be decided. From Figures 9 and 10, it can be inferred that voltage profile and THD (%) of the real power at bus 10 are found to be worst with existing methods such as harmony search algorithm [4], ant colony algorithm [9], and big-bang–crunch method [30] for both CPLF and CILF. Therefore, D-STATCOM is placed at bus 10. Figures 17 and 18 show the voltage (pu) comparisons at bus 10 for CPLF and CILF. It is also observed that switching of D-STATCOM with FLC improves its voltage profile and THD (%). This means that switching of D-STATCOM with FLC helps to improve the performance parameters in comparison to existing methods. The comparison of voltage profile and THD (%) of real power at bus 10 with existing techniques and D-STATCOM-based FLC is shown in Tables 17 and 18 and its graphical comparison is shown in Figures 19 and 20.

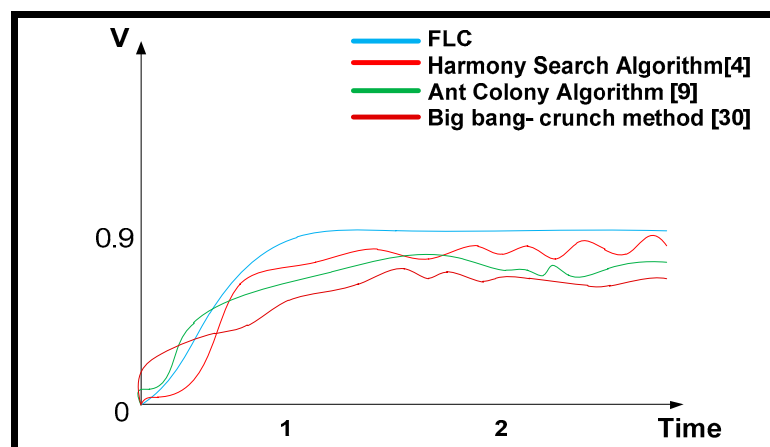


Figure 17. Voltage comparison at bus 10 for CPLF.

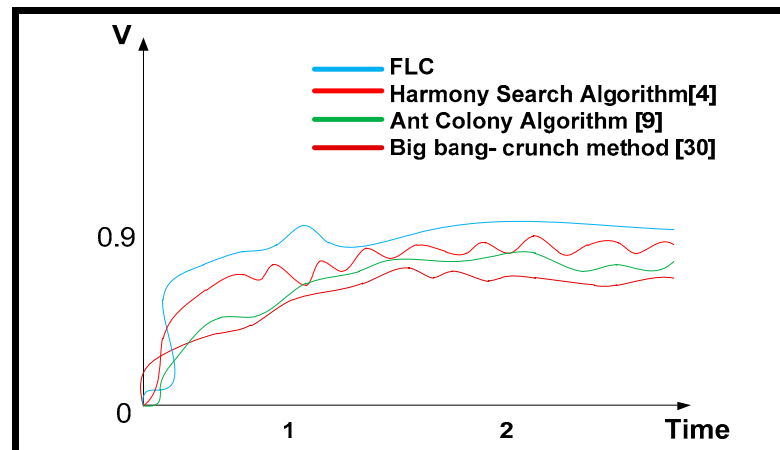


Figure 18. Voltage comparison at bus 10 for CILF.

Table 17. Comparative analysis for voltage (pu) at bus 10 for both types of load.

Load Type	FLC	D-STATCOM-Based FLC	Harmony Search Algorithm [4]	Ant Colony Algorithm [9]
CPLF	1	0.98	0.97	0.93
CILF	1.01	0.99	0.97	0.93

Table 18. Comparative analysis for THD (%) of real power at bus 10 for both types of load.

Load Type	FLC	D-STATCOM-Based FLC	Harmony Search Algorithm [4]	Ant Colony Algorithm [9]
CPLF	5.2	9.12	9.89	10.5
CILF	6.3	9.65	9.65	10.26

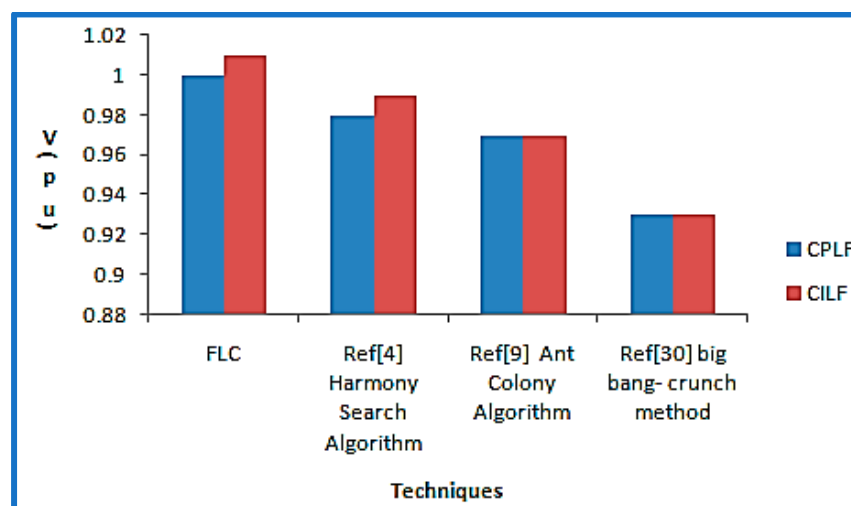


Figure 19. Graphical voltage comparison at bus 10 with different methods for CPLF and CILF.

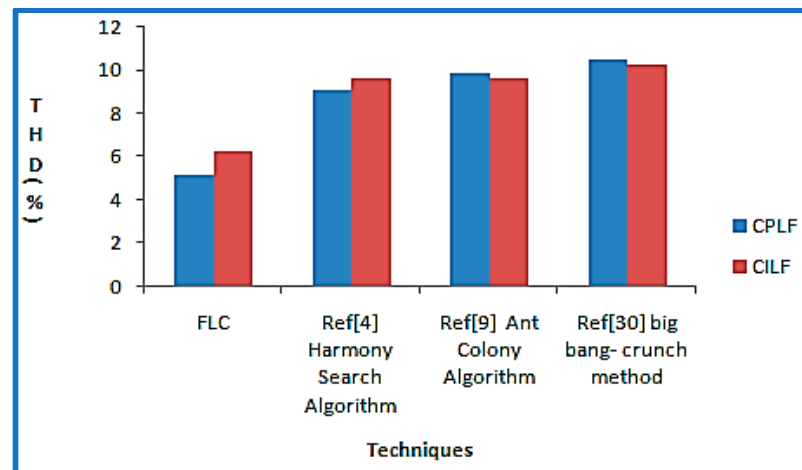


Figure 20. Graphical THD (%) of real power comparison at bus 10 with different methods for CPLF and CILF.

4. Result Summary

This article shows location and sizing of three DGs for CPLF and CILF types of load using GA and heuristic PDF method. The location of the DGs was obtained based on three different parameters such as line power losses, accuracy, and sensitivity. The application of GA method shows that all three parameters of DG placement are improved in comparison with the heuristic PDF method as well as existing methods such as ant-lion optimization algorithm, coyote optimizer, modified sine-cosine algorithm, and particle swarm optimization. It is also observed that after obtaining optimal location for DG placement at bus 17, optimal sizing for DG has been determined among all buses and the most optimal solution turns out to be at bus 17 in terms of minimum real and reactive power. It is found that determination of size of DG is quite satisfactorily observed under GA in comparison to the heuristic PDF method, ant-lion optimization algorithm, coyote optimizer, modified sine-cosine algorithm, and particle swarm optimization. Subsequently, bus 3 and bus 4 are the second and third best locations for placement of DGs with optimal size. Now, positioning of D-STATCOM on the IEEE 33 bus system is assessed in such a way that the bus with the worst performance in terms of THD and voltage profile has to be detected. On the basis of the analysis performed, bus 10 is found to be most suitable for locating the D-STATCOM. Afterwards, in order to improve the THD and voltage profile, switching of D-STATCOM is performed through FLC, consequently showing superiority over other existing methods. The current research will provide considerable expertise and also acts as a guide for researchers, including utility engineers, regarding problems to be addressed in order to optimize the size and position of DG units within electrical power systems. The metaheuristic computation approaches recently unveiled could be implemented for optimal design and fitting of DG in network delivery in future.

5. Conclusions

This article presents the optimal location and sizing of three DGs in the IEEE 33 bus test system by using the heuristic PDF method and GA for CPLF and CILF. Associated bus locations are examined for analysis of the impact of optimal placement and size of DG. The optimal locations of DGs are selected in terms of performance parameters such as line power losses, sensitivity, and accuracy while sizing of DG is obtained in terms of real and reactive power. It is evident that the parameters such as voltage profile, line power loss, accuracy, sensitivity, THD, etc. are improved with the GA method as compared to the heuristic PDF method and other existing methods such as the ant-lion optimization algorithm, coyote optimizer, modified sine-cosine algorithm, and particle swarm optimization. It is also confirmed that determining DG size is resolved quite satisfactorily with the GA method in terms of real power and reactive power, rather than heuristic PDF and other existing

methods. Further positioning of D-STATCOM is being decided on the basis of bus having the worst voltage profile and THD (%) of real power. The D-STATCOM is controlled with FLC which gives improved voltage and less THD of real power in comparison to existing techniques.

Author Contributions: Conceptualization, P. and M.S.; formal analysis, P., A.A. and S.S.M.G.; funding acquisition, S.S.M.G.; investigation, A.A.; methodology, P., M.S. and A.A.; project administration, P., A.A. and S.S.M.G.; resources, S.S.M.G.; software, P. and M.S.; supervision, P., A.S.S. and M.S.; validation, P. and M.S.; visualization, P., A.S.S., M.S. and A.A.; writing—original draft, P., A.S.S. and M.S.; writing—review and editing, P., A.A. and S.S.M.G. All authors have read and agreed to the published version of the manuscript.

Funding: This research was funded by TAIF UNIVERSITY RESEARCHERS SUPPORTING PROJECT, grant number TURSP-2020/34, Taif University, Taif, Saudi Arabia, and “The APC was funded by SHERIF GHONEIM”.

Data Availability Statement: All data generated or analysed during this study are included in this research article and any relevant information related to the current study are available from the corresponding author on reasonable request.

Acknowledgments: The authors would like to acknowledge the financial support received from Taif University Researchers Supporting Project Number (TURSP-2020/34), Taif University, Taif, Saudi Arabia.

Conflicts of Interest: The authors declare no conflict of interest.

Abbreviations

DG	Distributed generator	δ_i	Load angle
CPLF	Constant power load flow	θ_i	Impedance angle at ‘i’ bus
CILF	Constant impedance load flow	θ_j	Impedance angle at ‘j’ bus
FLC	Fuzzy logic controller	ε	Tolerance limit
GA	Genetic Algorithm	y'	Initial code of string
D-STATCOM	Distribution static compensator	λ	Difference between measured and reference power
THD	Total harmonic distortion	σ	Standard deviation
PDF	Probability distribution method	E	Error
PWM	Pulse width modulation	NB	Negative big
S_{ij}	Complex power between 2 buses i & j	NM	Negative medium
P_{ij}	Real power between 2 buses i & j	NS	Negative small
Q_{ij}	Reactive power between 2 buses i & j	PB	Positive big
S_{loss}	Complex power loss	PM	Positive medium
G_{ij}	Conductance between i & j bus	PS	Positive small
B_{ij}	Susceptance between ‘i’ & ‘j’ bus	ZS	Zero

References

- Bernardon, D.P.; Mello, A.P.C.; Pfitscher, L.L.; Canha, L.N.; Abaide, A.R.; Ferreira, A.A. Real-time reconfiguration of distribution network with distributed generation. *Electr. Power Syst. Res.* **2014**, *107*, 59–67. [[CrossRef](#)]
- Chicco, G.; Mazza, A. An overview of the probability-based methods for optimal electrical distribution system reconfiguration. In Proceedings of the Fourth International Symposium on Electrical and Electronics Engineering (ISEEE), Galați, Romania, 11–13 October 2013; pp. 1–10.
- Chan, C.-M.; Liou, H.-R.; Lu, C.-N. Operation of distribution feeders with electric vehicle charging loads. In Proceedings of the 2012 IEEE 15th International Conference on Harmonics and Quality of Power (ICHQP), Hong Kong, China, 17–20 June 2012; pp. 695–700.
- Ganguly, S.; Samajpati, D. Distributed generation allocation on radial distribution networks under uncertainties of load and generation using genetic algorithm. *IEEE Trans. Sustain. Energy* **2015**, *6*, 688–697. [[CrossRef](#)]
- Martins, V.F.; Borges, C.L.T. Active distribution network integrated planning incorporating distributed generation and load response uncertainties. *IEEE Trans. Power Syst.* **2011**, *26*, 2164–2172. [[CrossRef](#)]

6. Salman, N. Practical mitigation of voltage sag in distribution networks by combining network reconfiguration and DSTATCOM. In Proceedings of the IEEE International Conference on Power and Energy (PECON2010), Kuala Lumpur, Malaysia, 29 November–1 December 2010.
7. Li, G.; Shi, D.; Duan, X.; Li, H.; Yao, M. Multiobjective optimal network reconfiguration considering the charging load of PHEV. In Proceedings of the Power and Energy Society General Meeting, San Diego, CA, USA, 22–26 July 2012; IEEE: New York, NY, USA, 2012; pp. 1–8.
8. Pandi, V.R.; Zeineldin, H.H.; Xiao, W. Determining optimal location and size of distributed generation resources considering harmonic and protection coordination limits. *IEEE Trans. Power Syst.* **2013**, *28*, 1245–1254. [[CrossRef](#)]
9. Swarnkar, A.; Gupta, N.; Niazi, K.R. Optimal placement of fixed and switched shunt capacitors for large-scale distribution systems using genetic algorithms. In Proceedings of the Innovative Smart Grid Technologies Conf. Europe (ISGT Europe), Gothenburg, Sweden, 11–13 October 2010; IEEE: New York, NY, USA, 2010; pp. 1–8.
10. Farahani, V.; Vahidi, B.; Abyaneh, H.A. Reconfiguration and capacitor placement simultaneously for energy loss reduction based on an improved reconfiguration method. *IEEE Trans. Power Syst.* **2012**, *27*, 587–595. [[CrossRef](#)]
11. Tuladhar, S.R.; Singh, J.G.; Ongsakul, W. Multi-objective approach for distribution network reconfiguration with optimal DG power factor using NSPSO. *IET Gener. Transm. Distrib.* **2016**, *10*, 2842–2851. [[CrossRef](#)]
12. Jasthi, K.; Das, D. Simultaneous distribution system reconfiguration and DG sizing algorithm without load flow solution. *IET Gener. Transm. Distrib.* **2017**, *12*, 1303–1313. [[CrossRef](#)]
13. Kalambe, S.; Agnihotri, G. Loss minimization techniques used in distribution network: Bibliographical survey. *Renew. Sustain. Energy Rev.* **2014**, *29*, 184–200. [[CrossRef](#)]
14. Muhammad, M.A.; Mokhlis, H.; Naidu, K.; Franco, J.F.; Illias, H.A.; Wang, L. Integrated data base approach in multi-objective network reconfiguration for distribution system using discrete optimisation techniques. *IET Gener. Transm. Distrib.* **2018**, *12*, 976–986. [[CrossRef](#)]
15. Lalitha, M.P.; Reddy, V.V.; Usha, V. Optimal Dg placement for minimum real power loss in radial distribution system using PSO. *J. Theor. Appl. Inf. Technol.* **2010**, *13*, 107–116.
16. Gözel, T.; Hocaoglu, M.H. An analytical method for the sizing and siting of distributed generators in radial systems. *Electr. Power Syst. Res.* **2009**, *79*, 912–918. [[CrossRef](#)]
17. Zhang, S.; Cheng, H.; Li, K.; Bazargan, M.; Yao, L. Optimal siting and sizing of intermittent distributed generators in distribution system. *IEEJ Trans. Electr. Electron. Eng.* **2015**, *10*, 628–635. [[CrossRef](#)]
18. Kumar, K.S.; Jayabarathi, T. Power system reconfiguration and loss minimization for a distribution systems using bacterial foraging optimization algorithm. *Int. J. Electr. Power Energy Syst.* **2012**, *36*, 13–17. [[CrossRef](#)]
19. Kaur, M.; Ghosh, S. Network reconfiguration of unbalanced distribution networks using fuzzy-firefly algorithm. *Appl. Soft Comput.* **2016**, *49*, 868–886. [[CrossRef](#)]
20. Hung, D.Q.; Mithulanathan, N. Multiple distributed generator placement in primary distribution networks for loss reduction. *IEEE Trans. Ind. Electron.* **2013**, *60*, 1700–1708. [[CrossRef](#)]
21. Angelim, J.H.; Affonso, C.M. Impact of distributed generation technology and location on power system voltage stability. *IEEE Latin Am. Trans.* **2016**, *14*, 1758–1765. [[CrossRef](#)]
22. Wu, Y.-K.; Lee, C.-Y.; Liu, L.-C.; Tsai, S.H. Study of reconfiguration for the distribution system with distributed generators. *IEEE Trans. Power Deliv.* **2010**, *25*, 1678–1685. [[CrossRef](#)]
23. Liu, K.-Y.; Sheng, W.; Liu, Y.; Meng, X. A network reconfiguration method considering data uncertainties in smart distribution networks. *Energies* **2017**, *10*, 618. [[CrossRef](#)]
24. Rao, R.; Ravindra, K.; Satish, K.; Narasimham, S.V.L. Power loss minimization in distribution system using network reconfiguration in the presence of distributed generation. *IEEE Trans. Power Syst.* **2013**, *28*, 317–325. [[CrossRef](#)]
25. Prabha, D.R.; Jayabarathi, T.; Umamageswari, R.; Saranya, S. Optimal location and sizing of distributed generation unit using intelligent water drop algorithm. *Sustain. Energy Technol. Assess.* **2015**, *11*, 106–113. [[CrossRef](#)]
26. Rezk, H.; Abdelkareem, M.A.; Ghenai, C. Performance evaluation and optimal design of stand-alone solar PV-battery system for irrigation in isolated regions: A case study in Al Minya (Egypt). *Sustain. Energy Technol. Assess.* **2019**, *36*, 100556. [[CrossRef](#)]
27. El-Zonkoly, A.M. Optimal placement of multi-distributed generation units including different load models using particle swarm optimization. *Swarm Evol. Comput.* **2011**, *1*, 50–59. [[CrossRef](#)]
28. Naik, S.G.; Khatod, D.K.; Sharma, M.P. Optimal allocation of combined DG and capacitor for real power loss minimization in distribution networks. *Int. J. Electr. Power Energy Syst.* **2013**, *53*, 967–973. [[CrossRef](#)]
29. Sandeep, K.; Ganesh, K.; Jaydev, S. A MINLP technique for optimal placement of multiple DG units in distribution systems. *Electr. Power Energy Syst.* **2014**, *63*, 609–617.
30. Othman, M.M.; Walid, E.; Yasser, G.H.; Almoataz, Y.A. Optimal placement and sizing of distributed generators in unbalanced distribution systems using supervised big bang-big crunch method. *IEEE Trans. Power Syst.* **2015**, *30*, 911–919. [[CrossRef](#)]
31. Naresh, A.; Mahat, P.; Mithulanathan, N. An analytical approach for DG allocation in primary distribution network. *Int. J. Electr. Power Energy Syst.* **2006**, *28*, 669–678.
32. Mithulanathan, N.; Oo, T.; Phu, L.V. Distributed generator placement in power distribution system using genetic algorithm to reduce losses. *TIJSAT* **2004**, *9*, 55–62.

33. Hamed, S.H. Intelligent water drops algorithm: A new optimization method for solving the multiple knapsack problem. *Int. J. Intell. Comput. Cybern.* **2008**, *1*, 193–212.
34. Muqbel, A.; Elsayed, A.H.; Abido, M.A.; Mantawy, A.A.; Al-Awami, A.T.; El-Hawary, M. Optimal Sizing and Location of Solar Capacity in an Electrical Network Using Lightning Search Algorithm. *Electr. Power Compon. Syst.* **2020**, *47*, 1247–1260. [[CrossRef](#)]
35. Siahbalaee, J.; Rezanejad, N.; Gharehpetian, G.B. Reconfiguration and DG Sizing and Placement Using Improved Shuffled Frog Leaping Algorithm. *Electr. Power Compon. Syst.* **2020**, *47*, 1475–1488. [[CrossRef](#)]
36. Baran, M.E.; Wu, F.F. Network reconfiguration in distribution systems for loss reduction and load balancing. *IEEE Trans. Power Deliv.* **1989**, *4*, 1401–1407. [[CrossRef](#)]
37. Bagherinezhad, A.; Palomino, A.D.; Li, B.; Parvania, M. Spatio-Temporal Electric Bus Charging Optimization with Transit Network Constraints. *IEEE Trans. Ind. Appl.* **2020**, *56*, 5741–5749. [[CrossRef](#)]
38. Elmetwaly, A.H.; Eldesouky, A.A.; Sallam, A.A. An Adaptive D-FACTS for Power Quality Enhancement in an Isolated Microgrid. *IEEE Access* **2020**, *8*, 57923–57942. [[CrossRef](#)]
39. Castiblanco-Pérez, C.M.; Toro-Rodríguez, D.E.; Montoya, O.D.; Giral-Ramírez, D.D. Optimal Placement and Sizing of D-STATCOM in Radial and Meshed Distribution Networks Using a Discrete-Continuous Version of the Genetic Algorithm. *Electronics* **2021**, *10*, 1452. [[CrossRef](#)]
40. Yuvaraj, T.; Devabalaji, K.; Ravi, K. Optimal Placement and Sizing of DSTATCOM Using Harmony Search Algorithm. *Energy Procedia* **2015**, *79*, 759–765. [[CrossRef](#)]
41. Rukmani, D.K.; Thangaraj, Y.; Subramaniam, U.; Ramachandran, S.; Madurai Elavarasan, R.; Das, N.; Baringo, L.; Imran Abdul Rasheed, M. A New Approach to Optimal Location and Sizing of DSTATCOM in Radial Distribution Networks Using Bio-Inspired Cuckoo Search Algorithm. *Energies* **2020**, *13*, 4615. [[CrossRef](#)]
42. Moayedi, H.; Mosavi, A. Synthesizing Multi-Layer Perceptron Network with Ant lion Biogeography-Based Dragonfly Algorithm Evolutionary Strategy Invasive Weed and League Champion Optimization Hybrid Algorithms in Predicting Heating Load in Residential Buildings. *Sustainability* **2021**, *13*, 3198. [[CrossRef](#)]
43. Kamel, S.; Amin, A.; Selim, A. Application of coyote optimizer for Optimal DG Placement in Radial Distribution Systems. In Proceedings of the 2019 International Conference on Computer, Control, Electrical, and Electronics Engineering ICCCEEE, Khartoum, Sudan, 21–23 September 2019.
44. Qu, C.; Zeng, Z.; Dai, J.; Yi, Z.; He, W. A Modified Sine-Cosine Algorithm Based on Neighborhood Search and Greedy Levy Mutation. *Comput. Intell. Neurosci.* **2018**, *2018*, 4231647. [[CrossRef](#)]
45. Al-Masri, H.M.K.; Al-Sharqi, A.A.; Magableh, S.K.; Al-Shetwi, A.Q.; Abdolrasol, M.G.M.; Ustun, T.S. Optimal Allocation of a Hybrid Photovoltaic Biogas Energy System Using Multi-Objective Feasibility Enhanced Particle Swarm Algorithm. *Sustainability* **2022**, *14*, 685. [[CrossRef](#)]